NSK Technical Journal

Motion & Control

No.14 May 2003

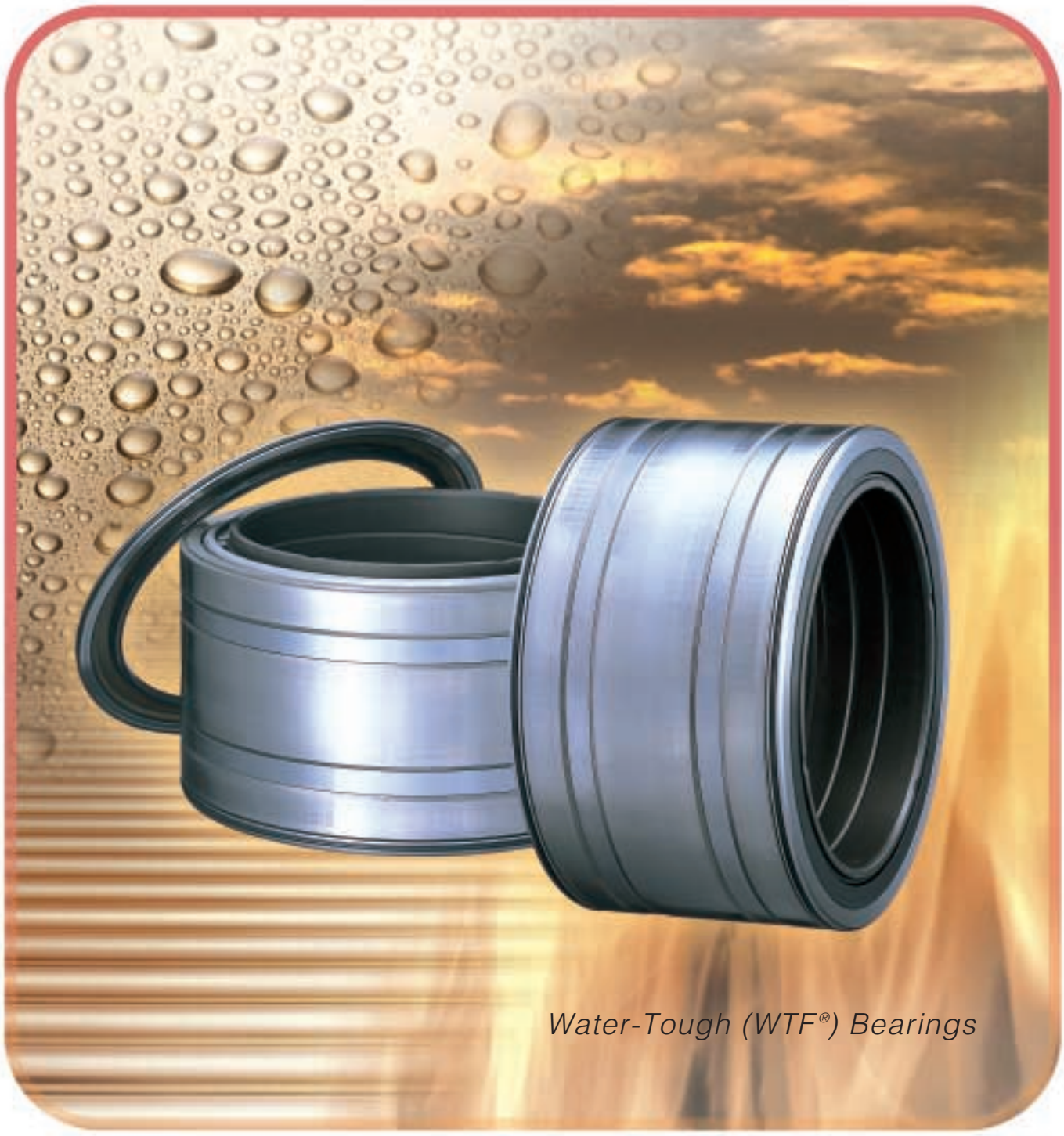

Water-Tough (WTF®) Bearings

ISSN1342-3630

NSK

MOTION & CONTROL No.14
NSK Technical Journal
Printed and Published: May 2003
ISSN1342-3630
Publisher: NSK Ltd., Ohsaki, Shinagawa, Tokyo, JAPAN
Public Relations Department
TEL +81-3-3779-7051
FAX +81-3-3779-7431
Editor: Tadao INOMATA
Managing Editor: Seizo SAITO
Design, Typesetting & Printing: Fuji Ad. Systems Corp.

Cover photos: Water-Tough (WTF®) Bearings

NSK Technical Journal
Motion & Control
No. 14
May 2003

NSK

Contents

Development of Water-Tough (WTF®) Bearings for Steel Mills
—Longer Life in Harsh Environments

Yoichi Matsumoto
Corporate Research and Development Center

ABSTRACT

NSK contributes to energy saving through bearing life extension. This report introduces that NSK has developed Water Tough Bearing (WTF® bearing), which has longer life than conventional bearings under water-infiltrated lubrication such as in steel mill.

To understand the mechanism of water-induced flaking and thereby enable countermeasures to be devised, the analyses of past experiments, including bearings that actually failed in services were carried out. In addition, fatigue life test methods that reproduce short life under water-infiltrated lubrication were developed. Using these methods it was possible to observe the flaking process precisely and to study what material parameters affect the bearing life. It was found that failure under water-infiltrated lubrication initiated from non-metallic inclusions on the rolling contact surface. The fatigue crack propagation was initially intergranular and then changed to transgranular, eventually resulting in flaking. Higher cleanliness, which means less failure initiation sites, and nickel, which strengthens the grain boundaries, were found to improve bearing life under water-infiltrated lubrication. Water Tough Bearing material has such the higher cleanliness and stronger grain boundaries.

1. Introduction

Operating conditions of roll neck bearings at steel mills include water-infiltrated lubrication and the ingress of foreign particles, such as scale, which can cause flaking of rolling contact surfaces of the bearings. Such an operating environment is no doubt very harsh. NSK bearings are designed for use in such harsh environments with tight seals on both sides[1] to prevent grease outflow and to prevent ingress of water and foreign particles. Today's needs of steel mills, however, demand greater sealing performance.

Failed bearings are sent as scrap to a melting furnace to be reused as raw material for steel products. This recycling system is so well established that our bearings have long been contributing to an appreciable level of energy savings. For greater energy savings, however, it is important to lengthen the bearing recycling intervals by extending bearing service life that has been terminated by flaking. In light of this, NSK has developed a water-tough (WTF®) bearing material that achieves longer bearing life for roll necks used at steel mills, as reported in the following sections.

2. Primary Objectives of Development

We developed the WTF® bearing with the primary objectives of:

(1) Determining what the flaking mechanism is for bearings under water-infiltrated lubrication;
(2) Establishing fundamental improvements based on such findings; and
(3) Extending the actual service life of bearings in the field by at least twofold.

To meet our objectives, we thoroughly examined bearings that had failed in the field. We then built a testing machine capable of simulating bearing flaking under water-infiltrated lubrication in the field, analyzed the flaking process in detail, and identified the fatigue life-relevant elements. We then tested our newly developed WTF® bearings in the laboratory and in the field. Results of our analysis, which validate the effectiveness of this product, are discussed here.

3. Flaking Mechanism under Water-Infiltrated Lubrication

If bearing lubricants, such as oil or grease, could remain free of contamination, fatigue life would be 20 to 100 times as long as its theoretical life[2], and would have no problems related to fatigue life. According to fatigue life theory[3], flaking originates from nonmetallic inclusions (a material defect) slightly below the rolling contact surface of the bearing material. Such a flaking mechanism was experimentally proven to be correct by the authors[4]. Fig. 1 shows schematically the mechanism of flaking under uncontaminated lubrication, and Fig. 2 shows a nonmetallic inclusion from which flaking actually originated, which was an alumina type inclusion located in the center of the spalling area.

Our tests[5] verify that under water-only lubricated conditions, flaking does not occur, but rather abrasion takes place. What would the failure morphology be if

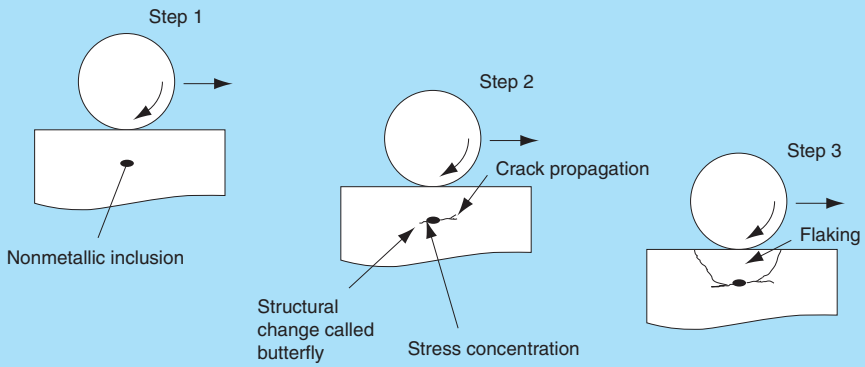

Fig. 1 Flaking mechanism under clean lubrication

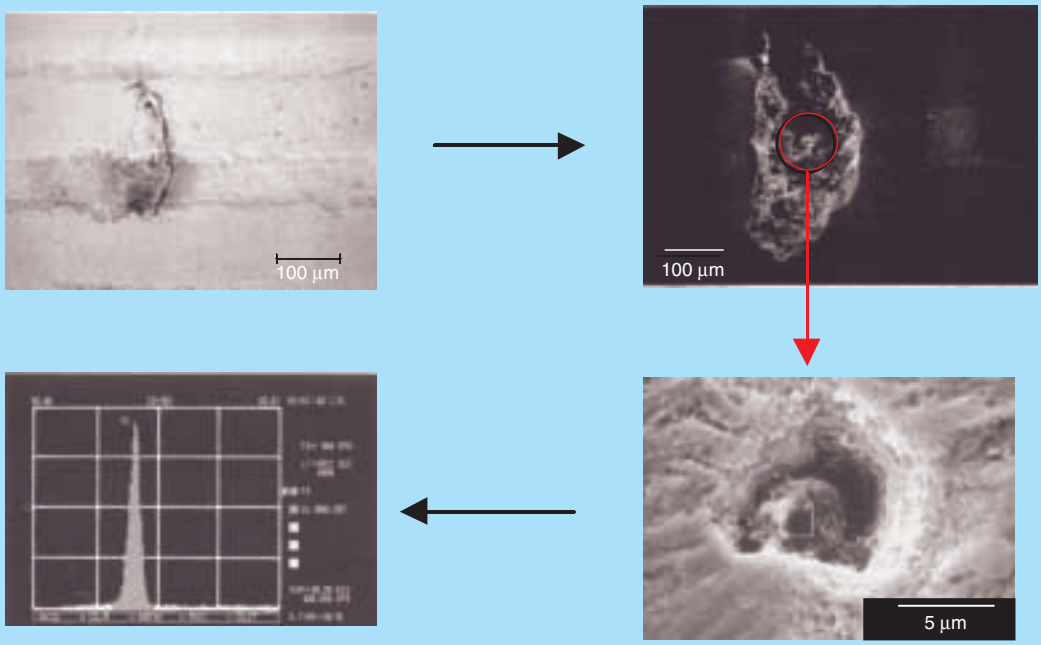

Fig. 2 Origin of flaking due to a nonmetallic inclusion

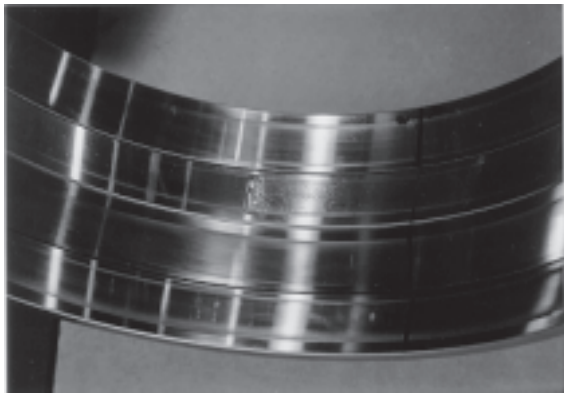

Fig. 3 Failed roll neck bearing from the field

water were added to oil or grease lubricant? Fig. 3 shows an outer ring of a roll neck bearing that experienced failure in the field. The failure type is flaking. The flaking location of roll neck bearings in steel mills is often at a load zone of outer rings.

What is the initiation of flaking under water-infiltrated lubrication? We observed early-stage flaking of the outer rings of roll neck bearings that failed in the field (Fig. 4). This flaking has a small pit in the raceway surface, with a crack running inwards. Thus flaking originated in the raceway surface. As mentioned earlier, under ideal lubrication, flaking originates from nonmetallic inclusions located slightly below the raceway surface. Then, under water-infiltrated lubrication, from what in the raceway

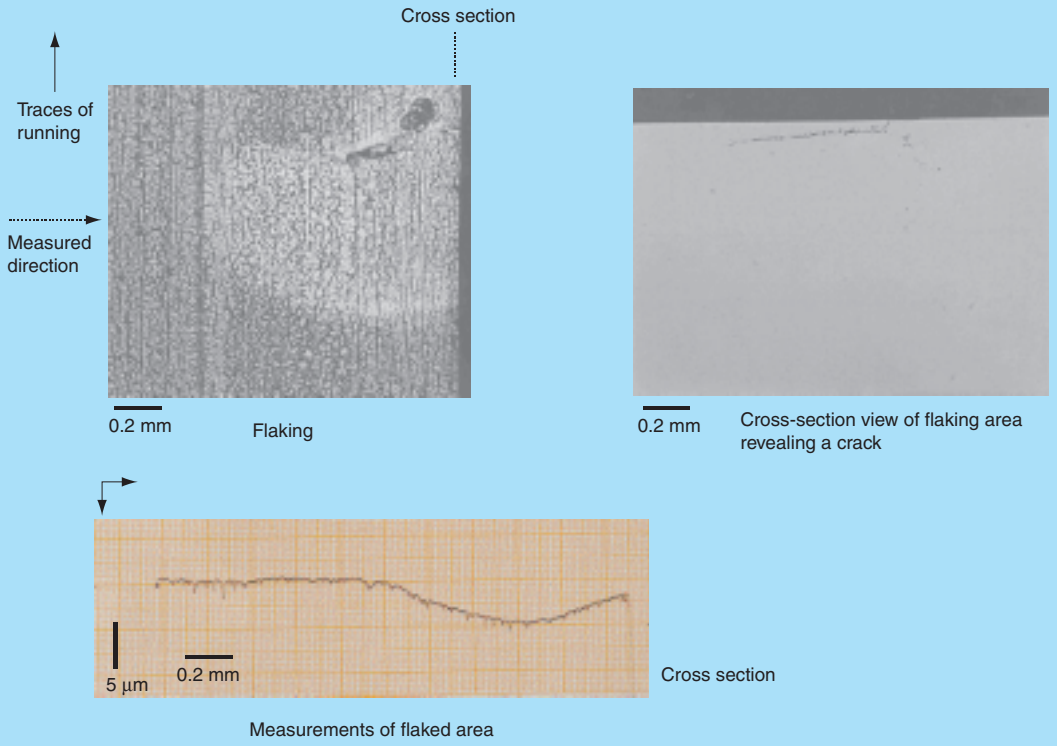

Fig. 4 Water-induced flaking in early stage in service

Table 1 Test Conditions

Test bearings	Tapered roller bearing (ø85 × ø130 × 30 mm)	Thrust ball bearing (ø25 × ø52 × 18 mm)
Water infiltration rate	20 mℓ/7h	30 mℓ/24h
Lubricant	Lithium soap grease (60g)	VG10 oil (70 mℓ)
P/C	0.25	0.35
Running speed	1500 min^{-1}	1250 min^{-1}

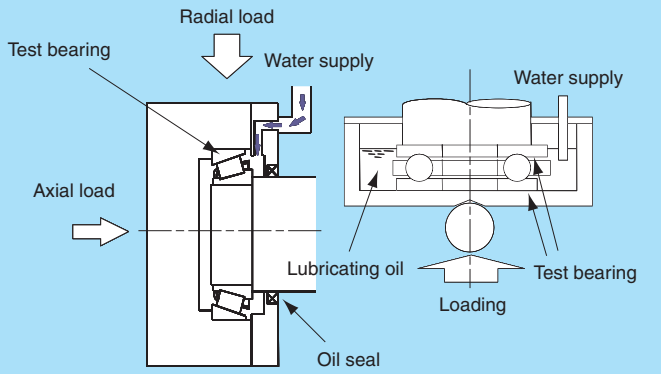

Fig. 5 Testing machine arrangements for reproducing flaking under water-infiltrated lubrication (Roller bearing / Ball bearing)

surface does flaking originate?

To solve this question, we built a testing apparatus (Fig. 5) in the laboratory that was capable of simulating field conditions (Table 1) and reproducing water-induced flaking. Grease-lubricated tapered roller bearings were used as test bearings. Roll neck bearings for work rolls in the field usually such bearings. In addition, ball bearings under oil and water-infiltrated lubrication were also tested to provide a minute observation of flaking and a greater number of test results.

Throughout these two tests, we observed the process of flaking. We identified the early stages of flaking of the tapered roller bearings under grease and water-infiltrated lubrication (Fig. 6). Cracks nucleated from the pits and then propagated deeper into the subsurface area. Both field roll neck bearings and experimental room test results show that flaking mostly occurs in the load zones of the outer rings. To analyze how the pits in the raceway surface are made, we conducted a study using bearings whose rings were made of martensitic stainless steel and super-clean steel to see if pits in the raceway surface were caused by corrosion or by nonmetallic inclusions on the surface.

Fig. 7 shows the fatigue life test results of bearings. One bearing consisted of martensite stainless steel rings; the other bearing consisted of standard 52100 steel rings. The fatigue life of highly corrosion-resistant martensitic stainless steel showed no improvements over that of standard bearing steel AISI52100. This means that the

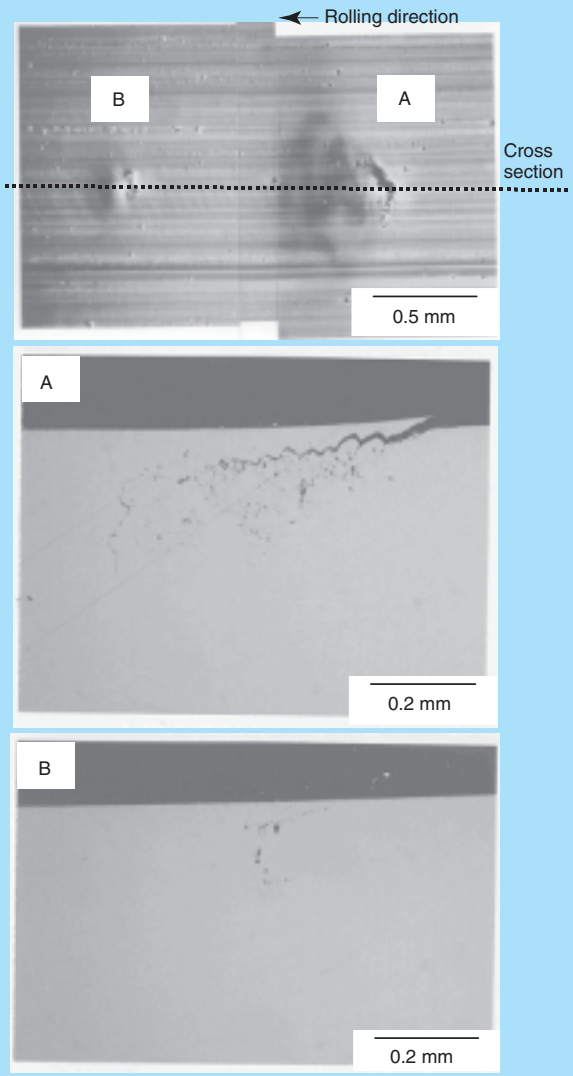

Fig. 6 Early stage flaking of the outer ring raceway of a tapered roller bearing under water-infiltrated grease lubrication

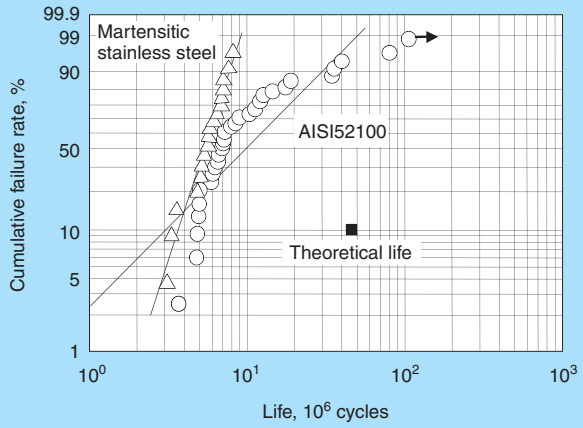

Fig. 7 Influence of corrosion resistance upon fatigue life under water-infiltrated lubrication

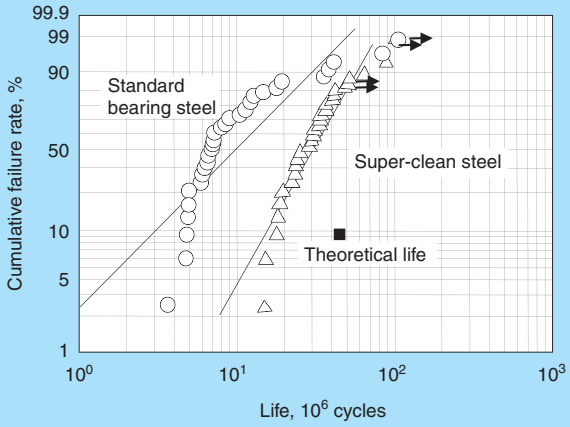

Fig. 8 Influence of steel cleanliness upon fatigue life under water infiltrated lubrication

pits in the raceway surface are not caused by corrosion.

Fig. 8 shows the fatigue life results of bearings. One bearing consisted of super-clean steel rings; the other bearing consisted of standard 52100 steel rings. Fatigue life of the super-clean steel was three times longer than that of the standard 52100 bearing steel. This would suggest that spalling of nonmetallic oxide inclusions caused the formation of pits in the raceway surface.

The mechanism of flaking of bearings under water-infiltrated lubrication is illustrated in Fig. 9. Under water-infiltrated lubrication, oil film formation between the rolling elements and the rings was insufficient, which eventually resulted in wear of the rolling contact surfaces. For roll neck bearings, the load zone of the outer ring is the most severe because the number of stress cycles and wear depth is the maximum of the bearing. This means that the flaking occurs in this region. As the wear of the raceway surface develops, oxide inclusions become protrusive and become points of stress concentration. High contact stresses eventually cause cracks. If no water is present in the lubricant, such early cracking will not take place because of the high fatigue strength of steel. However, if water is present in the lubricant, the fatigue strength of steel is reduced, giving rise to this phenomenon. This is similar to the significant reduction in fatigue limit[6] seen in rotating bending fatigue tests conducted in water and steam environments. The oxide inclusions that have acted as stress concentration points will flake off in the course of time, while water will infiltrate into the cracks. Cracking will develop faster in the presence of water than when no water is present, eventually causing failure. Cracking takes place at the matrix in contact with nonmetallic inclusions. Microscopic observations reveal the first propagation of cracking is along grain boundaries where the material strength is low in the presence of water[7].

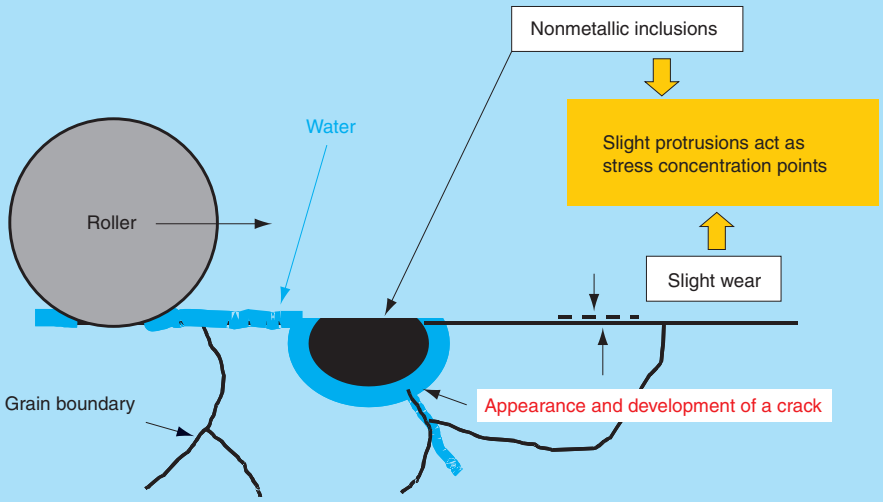

Fig. 9 Water-induced flaking

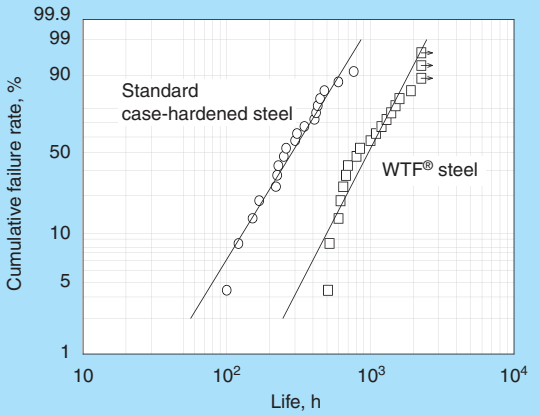

Water supply rate: 20 cc/7h
Fine iron powder (iron oxide) particle sizes: 32 µm, max.
P/*C*: 0.25

N = 1500 rpm
L_{10} cal: 1130h
Grease: Adrex

Fig. 10 Longer life of WTF® tapered roller bearing under grease lubrication contaminated with water and dust simulating actual service condition

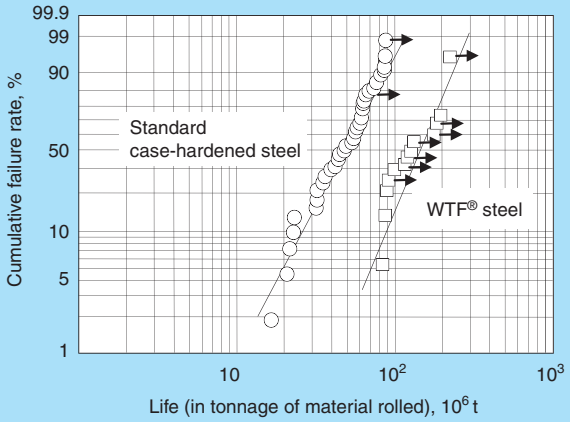

Fig. 11 Longer life of WTF® roll neck bearing used in cold strip mills

4. Features of WTF® Bearings

WTF® bearings are made of super-clean steel. The surface retained austenite content is controlled to an optimum level, which improves fatigue life under debris-contaminated lubrication. The stronger grain boundary is achieved by optimum alloy balance.

Fig. 10 shows the fatigue life results of the WTF® bearing operating under water-infiltrated grease lubrication and powder debris (iron oxide) contamination simulating actual operating conditions. Fig. 11 shows the test results from an actual cold strip mill. In both of these tests, the WTF® bearings showed a life approximately three times longer than bearings made of conventional case-hardened steel.

5. Conclusion

We have reported that WTF® bearings have achieved a life approximately three times longer than conventional bearings, as simulated tests in our laboratory and actual field applications demonstrate. Therefore, we believe that the use of this bearing in a harsh environment can contribute to further energy savings.

References:

1) K. Uchida, "Sealing and Cleanness Improvement of Four-Row Tapered Roller Bearings for Roll Necks," NSK Technical Journal, No. 639 (1980) 19-25.
2) K. Furumura et al., "Progress in Through-Hardening Bearing Steels: User's Experience," Bearing Steels: Into the 21st Century, ASTM STP 1327, J. J. C. Hoo and W. B. Green, Eds., American Society for Testing and Materials, West Conshohocken, PA, 1998, 249-264.
3) Lundberg, G. and Palmgren, A., "Dynamic Capacity of Rolling Bearings," Ingeniuörsvetenskapsakademiens Nr. 196 (1947).
4) Y. Matsumoto et al., "Application of Acoustic Emission Technique to Detection of Origin of Rolling Contact Fatigue," Proc. 6th Int. Conf., Mechanical Behavior of Materials, (1991), 667.
5) H. Sugi et al., "Life Characteristics of Thrust Ball Bearings in Water," NSK Technical Journal, No. 657 (1994) 22-27.
6) H. Ishii et al., "Effects of Structure and Environment of Eutectoid Steel on Its Fatigue," Japan Material Strength Society Journal, 17-3 (1983) 65-77.
7) Y. Matsumoto et al., "Rolling Contact Fatigue under Water-Infiltrated Lubrication," Bearing Steels, ASTM STP 1419, J. M. Beswick, Ed, American Society for Testing and Materials, West Conshohochen, PA, 2002.

Yoichi Matsumoto

Non-Magnetic and Highly Corrosion-Resistant Titanium Alloy Bearings

Koji Ueda, Hideyuki Uyama, Manabu Ohori
Corporate Research and Development Center

ABSTRACT

NSK has developed highly corrosion-resistant titanium alloy rolling bearings. Titanium alloy is a safer material for the environment and personnel than prior non-magnetic bearing material, such as beryllium copper alloy. Titanium alloy is free from noxious chemical elements unlike beryllium copper alloy. The hardness of this titanium alloy developed by NSK is about 500HV, which was achieved by optimizing the chemical composition of the alloy and heat treatment conditions. As a result of the higher hardness, in comparison to ordinary titanium alloy, NSK's newly developed titanium alloy can be utilized for bearings. Applications of non-magnetic and corrosion-resistant titanium alloy bearings include electron beam equipment and semiconductor manufacturing devices.

1. Introduction

Information technology has progressed rapidly during recent years. Although previously laser beam equipment was used for processing and inspecting patterns on semiconductor wafers, recently electron beam equipment has developed for these tasks, since the wavelength of electron beams is shorter than that of laser beams.

When magnetic rolling bearings used in wafer holders and wafer carriages rotate in the vicinity of an electron gun that emits electron beams, the magnetic fields around the bearings are affected. Electro-magnetic interference adversely affects the ability of electron beams to accurately process and inspect semiconductor wafers. For equipment that uses electron beams, therefore, materials with an extremely low magnetic permeability are required. To resolve this problem, NSK developed non-magnetic titanium alloy bearings for electron beam applications.

2. Features

2.1 Physical properties

Austenitic non-magnetic stainless steel, ceramics, and beryllium copper alloys are well-known, as non-magnetic bearing materials. Table 1 shows the physical properties of these materials in addition to NSK's newly developed non-magnetic titanium alloy.

Non-magnetic stainless steel has a magnetic permeability of 1.001 to 1.01, which is enough for it to become slightly magnetized. For example, austenitic stainless steel can be magnetized by martensitic transformation if it goes through plastic deformation. This makes non-magnetic stainless steel an unsuitable bearing material for electron beam equipment. Ceramics has a permeability of not more than 1.001, which makes it virtually non-magnetic. However, ceramics can become charged with electron beam irradiation due to the electrical insulating properties of ceramics. Beryllium copper alloy is conductive and non-magnetic. Recently, however, the use of beryllium copper alloy in bearings has been avoided since beryllium is highly toxic.

In comparison, a titanium alloy is best suited for bearings in electron beam equipment, due to its conductive and non-magnetic properties. In addition, when compared to non-magnetic stainless steel or beryllium copper alloy, titanium alloy has higher corrosion resistance and is lighter in weight with one-third less density. Different from beryllium copper alloy, titanium alloy is free of harmful elements and is no threat to the environment and human body. Unlike ceramics, titanium alloy is also more workable by machining or cutting.

2.2 Hardness

For many years, titanium alloy has received attention as a possible bearing material for special environments.

Table 1 Properties of various non-magnetic bearing materials

	Newly developed titanium alloy	Conventional titanium alloy	Non-magnetic stainless steel	Beryllium copper alloy	Ceramic (silicon nitride)
Specific permeability	1.001, max.	1.001, max.	1.001 ~ 1.01	1.001, max.	1.001, max.
Conductivity	Good	Good	Good	Good	Poor
Hardness (HV)	450 ~ 500	300 ~ 350	420 ~ 450	420 ~ 450	1 500 ~ 2 000
Linear expansion coefficient ($\times 10^{-6}$)	8.8	8.4	11	17.6	2.5 ~ 3.3
Young's modulus (GPa)	110	108	200	130	250 ~ 330
Density (g/cm^3)	5.0	4.5	7.7	8.3	3.2
Corrosion resistance (Room temp.)	Excellent	Good	Fair	Good	Excellent

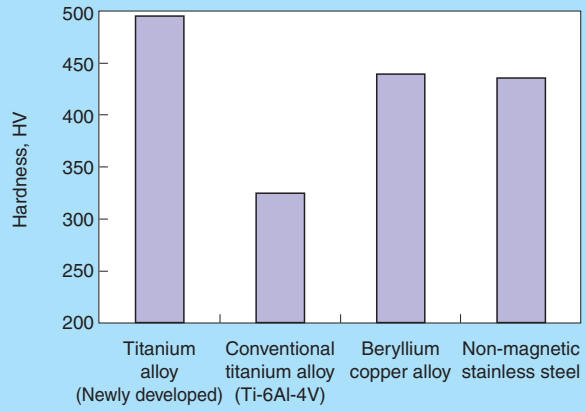

Fig. 1 Hardness of titanium alloy and non-magnetic materials

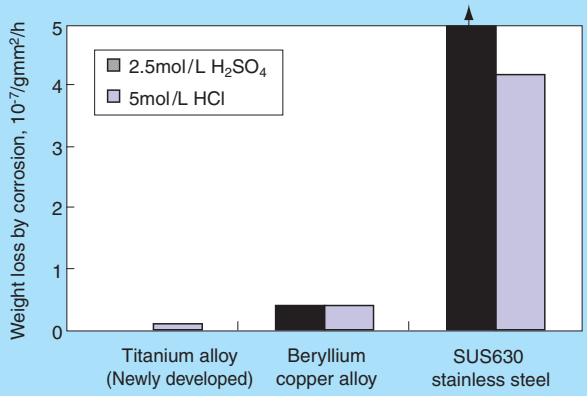

Fig. 2 Weight loss of new titanium alloy and beryllium copper alloy and stainless steel after immersion in sulfuric acid and hydrochloric acid

However, conventional titanium alloy, such as Ti-6Al-4V, is low in hardness with a hardness of 300 to 400 HV and is not applicable to rolling bearings that operate under high surface contact pressure conditions.

Fig. 1 shows the hardness of NSK's newly developed titanium alloy for bearings and conventional non-magnetic bearing materials. The hardness of this titanium alloy developed by NSK is about 500 HV. As a result of the higher hardness, NSK's newly developed titanium alloy, in contrast to conventional titanium alloy, can be utilized for rolling bearings.

Generally, a titanium alloy is hardened by the precipitation of fine αphase through the solution and aging treatment. By optimizing the chemical composition of the alloy and heat treatment conditions, NSK's newly developed titanium alloy for bearings has achieved maximum hardness among titanium alloys.

2.3 Corrosion resistance

The corrosion resistance of titanium alloy is the highest among structural metal materials. The corrosion resistance of titanium alloy, like stainless steel, is theoretically due to a passive film on the outside surface, but titanium's passive film is denser and tougher than that of stainless steel. Fig. 2 shows the results of a corrosion resistance test in a 2.5 mol/L sulfuric acid solution and a 5 mol/L hydrochloric acid solution at ambient temperatures. The corrosion resistance of the titanium alloy is much higher than that of SUS630 stainless steel and is even higher than that of beryllium copper alloy.

Among titanium alloys, our newly developed titanium alloy has outstanding corrosion resistance and exhibits exceptional resistance to oxidizing acids, reducing acids, and alkalis. This titanium alloy, however, is susceptible to corrosion by fluoric acids. The corrosion resistance of titanium alloy varies according to environmental conditions, such as operating temperatures and the types and concentrations of acids. Thus the operating environment for titanium alloy bearings needs to be carefully considered prior to use.

2.4 Load endurance

Fig. 3 shows the result of the load-induced flaking in the newly developed titanium alloy and a beryllium copper alloy. Table 2 shows the test conditions. In this test, the load was increased at regular intervals until flaking occurred.

Flaking of the beryllium copper alloy occurred at approximately 980N, while flaking of the newly developed titanium alloy occurred at about 2,600N. This proves that capacity of NSK's newly developed titanium alloy is higher than that of beryllium copper alloy.

Table 2 Test conditions

Rotational speed	1 000 min^{-1}
Test load	Incremental Started at 980N Increased in intervals: 392 ~ 784N/70 hours
Lubrication	Mineral oil bath (VG68)
Temperature	Room temp.
Rolling elements	AISI52100
Cage	Brass

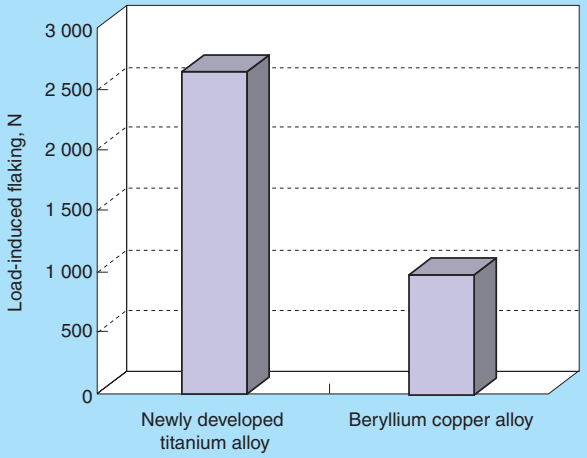

Fig. 3 Comparison of load-induced flaking on new titanium alloy and beryllium copper alloy

3. Performance and Specifications

Fig. 4 shows the endurance life test results of a 608 deep-groove ball bearing. Test bearings consisted of outer and inner rings made of the newly developed titanium alloy, ceramic (silicon nitride) balls, and a fluororesin cage. The test environment was under both atmospheric air and in a vacuum. Test results reveal trouble-free operations with excellent flaking life performance for a minimum of 10 million revolutions.

Bearings for electron beam equipment operate in a vacuum environment using a fluororesin cage, which requires no oil lubrication or packed grease. Depending on the operating conditions, bearings are treated with V-DFO lubricant film, resulting in stable operations even under heavy loads. These types of bearings usually use ceramic balls for the rolling elements. In cases where the entire bearing is required to have conductivity, rolling element surfaces are coated with a conductive film.

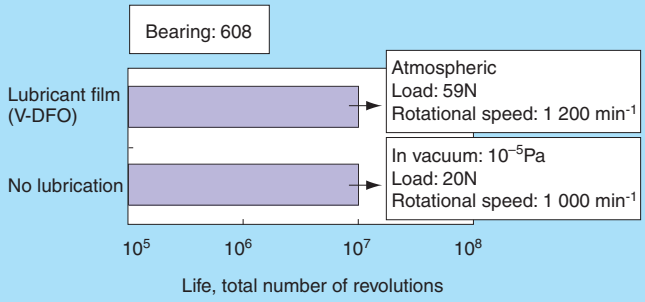

Fig. 4 Endurance life of non-magnetic and highly corrosion-resistant titanium

4. Conclusion

This article has presented the technological trend of increasing demand for non-magnetic bearing materials to keep pace with the use of electron beams in semiconductor manufacturing equipment. We have also introduced NSK's newly developed non-magnetic titanium alloy bearings. Our newly developed titanium alloy is the best substitute for beryllium copper alloys used for electron-beam equipment for semiconductor manufacturing equipment involving electron beams. This material is also being introduced to new applications that require high corrosion resistance and lightweight features.


Koji Ueda


Hideyuki Uyama


Manabu Ohori

Development of New High-Capacity Cylindrical Roller Bearings

Takashi Murai and Osamu Fujii, Corporate Research and Development Center
Shinichi Tsunashima, Bearing Technology Center

ABSTRACT

NSK has developed new cylindrical roller bearings that provide longer life and higher reliability for various industrial machines. Compared to conventional bearings, these new bearings have almost twice the service life, which has been achieved by increasing bearing load capacity by 20 to 30 percent. These bearings are available in two Series: EW and EM. NSK offers the EW Series with a pressed steel cage, and the EM Series with a machined brass cage. Both cages have been designed for high strength, adding to a bearing that offers greater resistance to vibration and shock load during operations. Furthermore, these Series enjoy greater stability in roller positioning thanks to cage roller guides that are much more precise, which further promote quieter operations.

1. Introduction

Cylindrical roller bearings are used in many industrial machines because they have a higher load carrying capacity than ball bearings and are more suited for high-speed revolutions than other types of roller bearings. Improvements in industrial machinery are constantly being made. Progress in endurance, reliability, efficiency, and energy conservation, as well as size reductions, lighter weight, and greater maintenance-free performance, require that the rolling bearings used in them provide longer life and higher reliability.

NSK has thus developed two new Series of cylindrical roller bearings with nearly twice the service life by increasing their load carrying capacity by 20 to 30 percent over that of conventional bearings. These bearings are available in two Series: the EW Series with a pressed steel cage (Photo 1) and the EM Series with a machined brass cage (Photo 2). With specially designed high-strength cages, the EM and EW Series provide greater shock-load resistance and reduced vibrations. The cage incorporates roller guides that are designed with greater precision to increase roller stability, resulting in reduced noise levels by approximately 5 dB compared with that of conventional bearings.

This report describes NSK's EW and EM Series high-capacity cylindrical roller bearings, which contribute to the development of machines with greater endurance and smaller size, as well as satisfying today's environmental need for lower noise.

2. Development

Generally speaking, increasing the number of rollers, or using larger rolling elements, can increase the load carrying capacity of cylindrical roller bearings. At the same time, the main bearing dimensions, bore and outside diameters, must conform to international standards to ensure compatibility. To achieve higher load carrying capacity within given dimensions, it becomes necessary to design and develop a stronger cage.

We also know from research and development that improving accuracy of the roller guides of the cage enhances roller stability. Additional benefits are both lowered noise levels and less vibration of cylindrical roller bearings.

We have thus succeeded in developing a quieter bearing

Photo 1 EW Series cylindrical roller bearing

Photo 2 EM Series cylindrical roller bearing

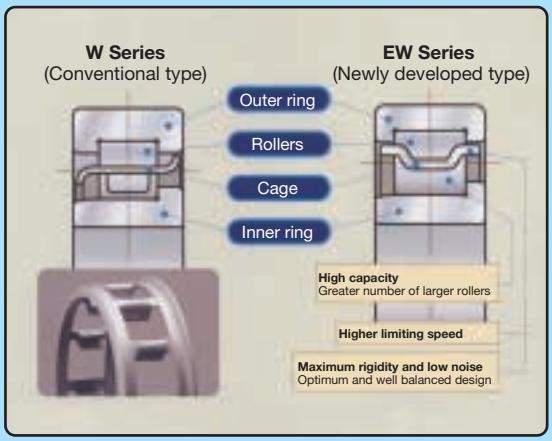

Fig. 1 Comparison between W and EW Series cylindrical roller bearing

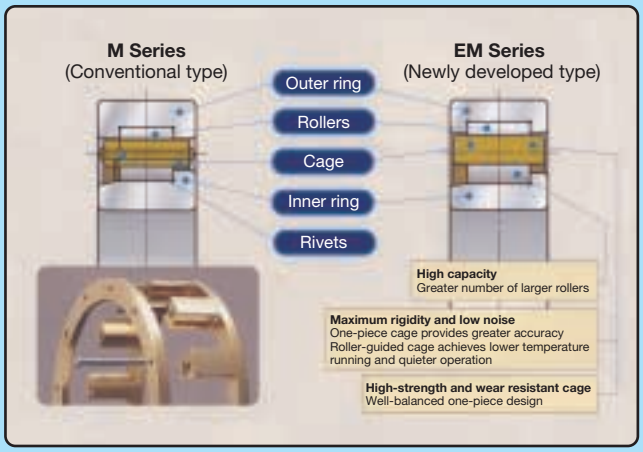

Fig. 2 Comparison between M and EM Series cylindrical roller bearing

with increased load capacity. This was achieved by a cage strength-enhancing design, and by refining the geometric accuracy of the cage roller guides, thus allowing for a greater number of larger rollers. Fig. 1 and 2 provide comparisons of NSK's conventional bearing series with the internal designs of the NSK EW Series high-capacity bearing, which uses a steel cage, and the NSK EM Series high-capacity bearing, which uses a machined brass cage.

Significant changes to conventional cage design play a major role in the enhancements made for these newly developed bearings. The pressed steel cage with flaps (W Series in Fig. 1 has been the standard steel cage that NSK has supplied to customers in the past. However, the W Series requires caulking of the flaps at the time of assembly, and its geometry imposes certain limitations on its application as a high-capacity cage. By contrast, the EW Series cage requires no caulking and is well balanced for high load-carrying capacity.

Fig. 2 shows the copper alloy, two-piece, ring-guided, rivet-type cage (M Series) that NSK has typically supplied to customers. While the M Series cages have been used in many of our bearings, they are not best suited for high-capacity bearings due to a rivet construction that limits cage bar dimensions. By contrast, the EM Series cage has a one-piece construction that provides enough strength for high-capacity bearings.

One-piece machined cages have been difficult to assemble and consequently have not been used for practical applications. NSK, however, has recently developed its own unique manufacturing technology and succeeded in mass-producing one-piece cages. With our manufacturing technology we can now manufacture high-strength cages, highly accurate roller guides, and ring guides.

3. Features

3.1 High capacity

The new cages used in EW and EM Series bearings allow for a greater number of larger rollers. The result is a basic dynamic load rating that is 20 to 30 percent higher than our conventional W and M Series bearings. This

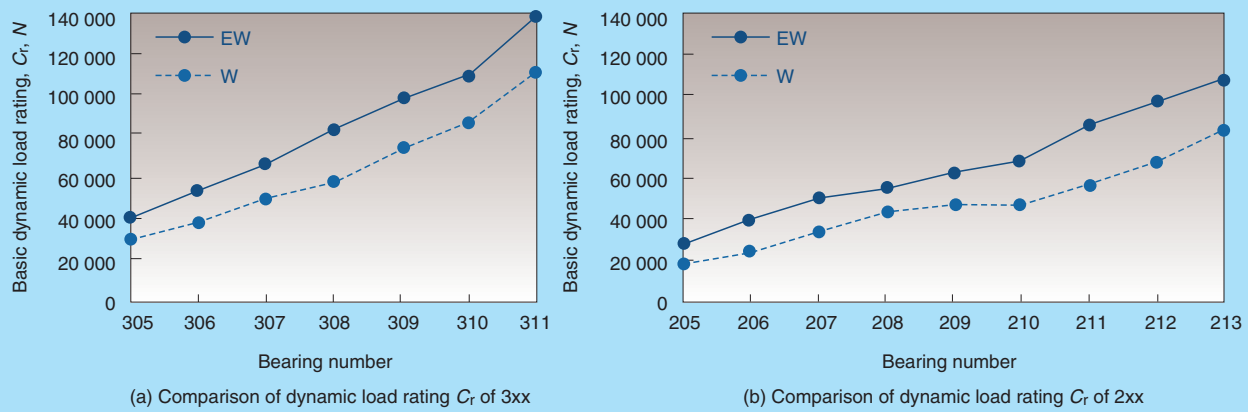

(a) Comparison of dynamic load rating C_r of 3xx

(b) Comparison of dynamic load rating C_r of 2xx

Fig. 3 Comparison of capacity between W and EW Series cylindrical roller bearing

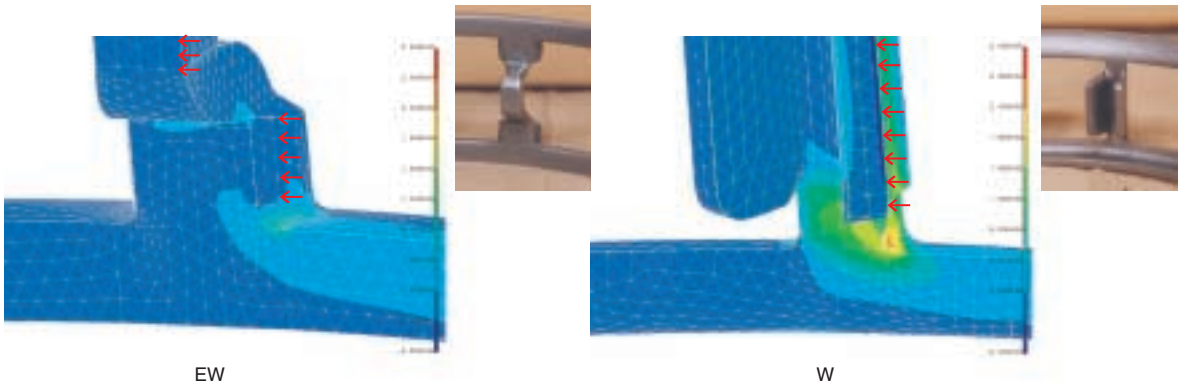

Fig. 4 Results of FEM analysis (W Series and EW Series)

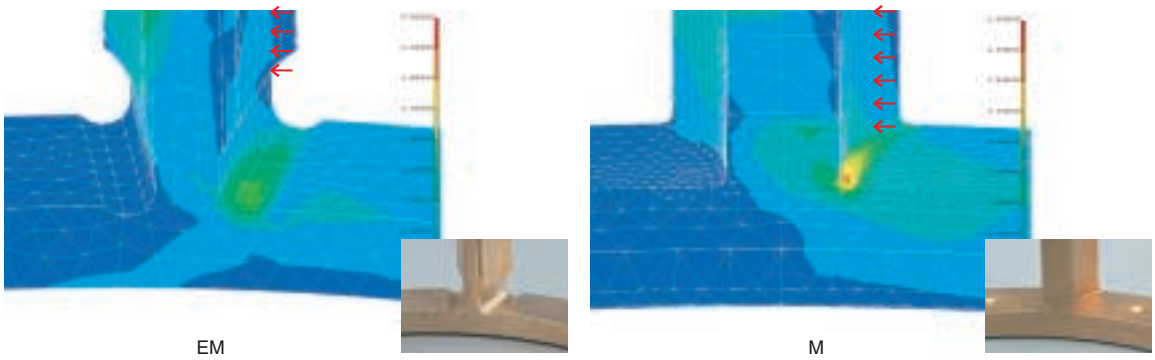

Fig. 5 Results of FEM analysis (M Series and EM Series)

higher rating is significant in that it also means the basic rated life of the EW and EM Series bearings is nearly doubled compared with conventional Series bearings operating under the same load conditions.

Main dimensions conform to ISO standards, thus facilitating international interchangeability. Fig. 3 provides comparisons of the basic load rating of the EW Series with that of conventional W Series bearings according to bearing sizes.

3.2 High-strength and highly accurate cages

Cage dimensions of the newly developed EW and EM Series cages[1), 2)] are theoretically designed and their strength is verified by tests under severe conditions. The new dimensions ensure optimum distribution of stress, which is caused by vibrations or shock load, throughout portions of the cage.

Fig. 4 and 5 reveal results of FEM analysis of maximum stresses in the cage bars of the steel cage and the machined brass cage, indicating that their maximum stresses are significantly lower than those of conventional types of cages. Specifically, the results of the FEM stress analysis indicate that the maximum stress of an EW Series steel cage is approximately 60% lower than that of a conventional W Series steel cage, and the maximum stress of an EM Series machined brass cage is approximately 50% lower than that of a conventional M Series machined brass cage.

The tests by which we evaluated and verified cage strength consisted of a drop impact test where the bearing assembly was dropped using a cam and spring for applying impact load to its cage, and an oscillation test in which the bearing was oscillated while being rotated at a high speed to apply impact load to its cage. Fig. 6 and 7 show the evaluation results of oscillation testing for the steel cage and machined copper cage. These results show that endurance of the EW Series steel cage was approximately 10 times higher than the W Series. As for the EM Series, our new brass cage remained intact throughout 10^8 oscillations, while rivets of the M Series brass cage became loose at 10^7 oscillations.

In addition, the high-strength material and high-precision pressing techniques used to manufacture the EW Series cages permit a 10 to 25 percent higher limiting speed than that of conventional W Series cages.

Roller guide accuracy of the EM Series cage is further

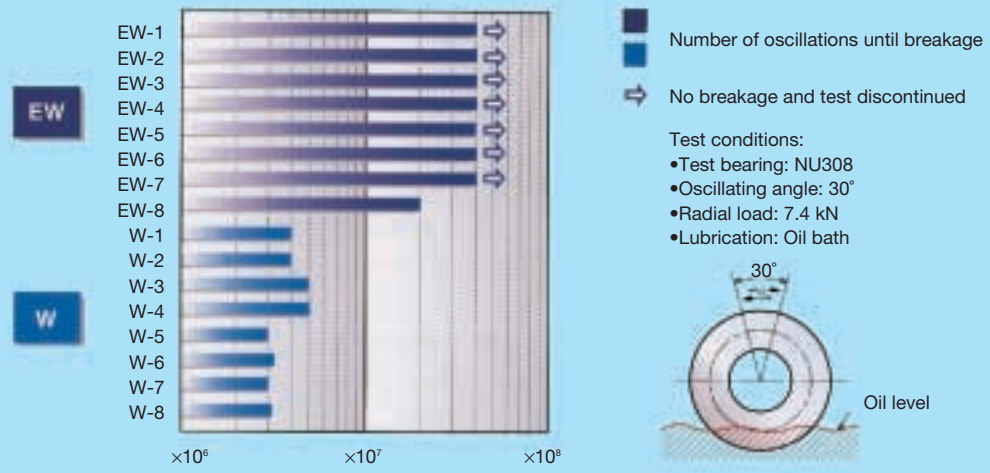

Fig. 6 Evaluation test results of cage strength for EW type

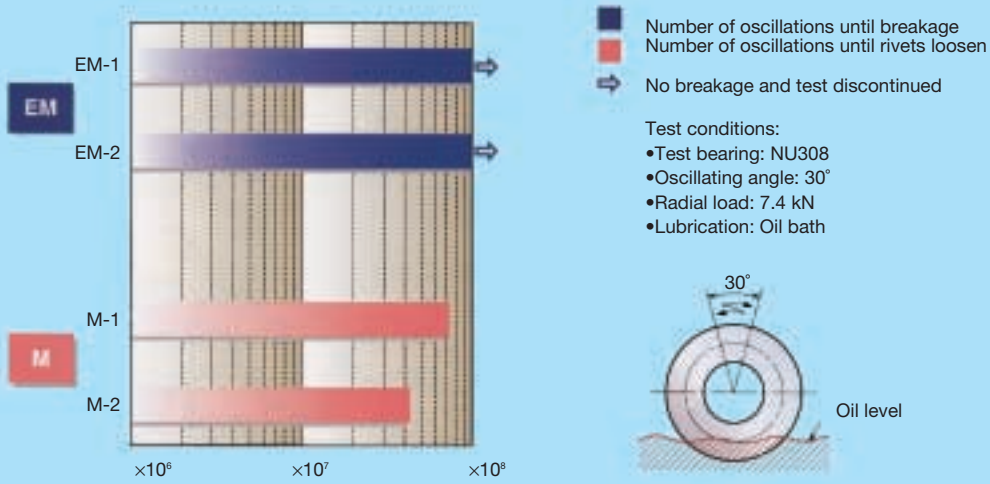

Fig. 7 Evaluation test results of cage strength for EM type

controlled to levels ranging from one-fourth to one-tenth of the M Series. Never before has the deviation of cage bars from rollers lengthwise in cage pockets been controlled to such highly accurate levels.

3.3 Low noise

Whereas the angular position of the cage affects the roller position inside the bearing, accuracy of the cage bars significantly affects the noise of cylindrical roller bearings (Fig. 8). Both the EW and the EM Series cages provide increased roller guide accuracy by using high-accuracy pressing processes (EW Series) or unique high-precision manufacturing processes (EM Series). Other noise prevention technologies[3), 4)] cultivated by our past research and developments are reflected in both cage designs.

Fig. 9 shows the results of EW and EM Series and bearing noise evaluations. This figure shows that the EW Series is 3 to 7 dB quieter than the conventional W Series, and that the EM Series is 6 to 8 dB quieter than the conventional M Series.

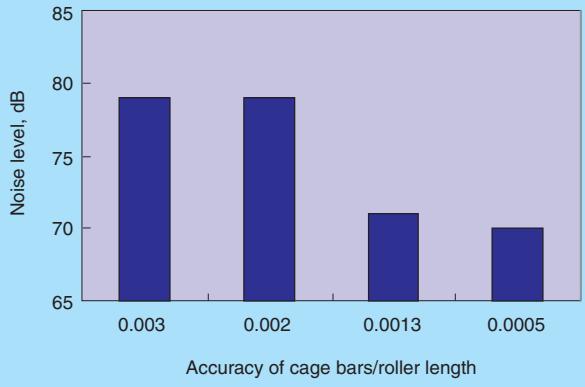

Fig. 8 Relation between cage accuracy and noise

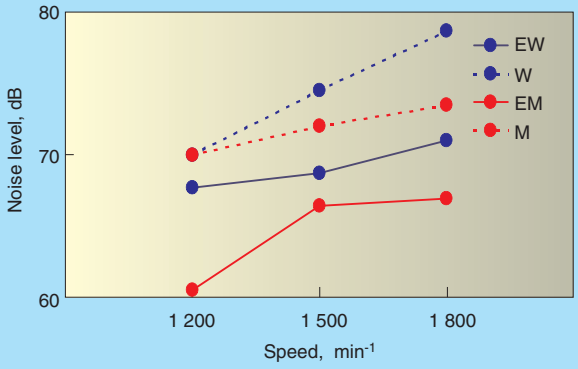

Measuring conditions:
Bearing number: NU308
Method: JIS B1548
Radial load: 392N
Speed: 1 200 to1 800 min^{-1}

Microphone position and measuring load

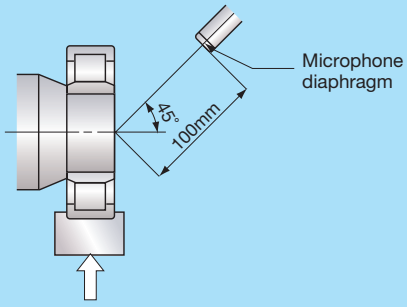

Fig. 9 Noise levels between EW and EM Series

4. Conclusion

We have introduced NSK's newly developed high-capacity cylindrical roller bearing EW and EM Series that provide customers with high load-carrying capacity and quieter operations. These high-performance bearing series are capable of sufficiently meeting high-capacity requirements while serving to reduce the size and weight of machines and equipment, as well as meeting low-noise requirements for machines and motors.

References:

1) NSK Report No. 535, "Cylindrical Roller Bearing EW Series," Studies on Machines, 53-10 (2001) 1062-1063.
2) NSK Report No. 533, "Cylindrical Roller Bearing EM Series," Studies on Machines, 53-8 (2001) 866-867.
3) T. Murai, "Squeak Noise Prevention Cylindrical Roller Bearing," NSK Technical Journal, No. 672 (2001) 68-72.
4) NSK Report No. 524, "Low-Noise Roller Bearing ZS Series for Motors," Studies on Machines, 52-11 (2000) 1166-1167.


Takashi Murai


Shinichi Tsunashima


Osamu Fujii

Super Precision Cylindrical Roller Bearings

Yoshiaki Katsuno, Corporate Research and Development Center
Osamu Iwasaki, NSK Precision Co.,Ltd.

ABSTRACT

Hard disk drive (HDD) components for personal computers and related IT products demand high precision during the manufacturing process. Requirements for precision and greater accuracy carry over into components of both advanced and general-purpose machinery for a variety of industries.

Conventionally, a general-purpose NC lathe is utilized in high-precision processing of general-purpose components by grinding a finish after cutting. However, an NC lathe machining center, or composition processor, that is capable of providing finished-grade work during the cutting process is anticipated by manufacturing systems that experience a short-term cycle of product design, or where there are significant changes in production quantities.

This paper introduces the super precision cylindrical roller bearings that are developed especially for main spindles with high-rigidity and high-load capacity aiming at high precision of these general-purpose types of multi-function machine tools.

1. Introduction

Manufacturing of small parts used in hard disk drives and IT-related components requires a machine tool spindle that can achieve a high degree of roundness, high dimensional accuracy, smoothness of the worked surface area, and holes with minimal deviation from roundness. IT-related parts, for instance, require a roundness of 0.2 µm.

In addition to demand for greater accuracy for such advanced machine parts, greater accuracy requirements for general industrial machinery are also on the rise. Until quite recently, high-accuracy processing of general machine parts by cutting was accomplished with a general-purpose NC lathe, followed by grinding. Nowadays, however, with product design changes being made in shorter periods and various products being produced in smaller quantities, there is an increasing demand for NC lathes, machining centers, and complex machines that can perform both cutting and finishing.

At NSK, we have developed super precision cylindrical roller bearings that are capable of satisfying requirements for high-accuracy of such general-purpose multifunction machine tools, and are especially suited for high rigidity and high-capacity spindles.

2. Functions Required for Machine Tool Spindles

Required major functions of current machine tool spindles include high-speed, high-precision, and high rigidity performance capabilities. In machining centers, many of the component machine tools require ultra high-speed performance for manufacturing aircraft parts and turbine blades. General-purpose machine tools, especially NC lathes, have double-row cylindrical roller bearings and thrust angular-contact ball bearings placed on the front side of a high-rigidity spindle. Using an NSK cartridge spindle, we tested and evaluated NSK's newly developed super precision cylindrical roller bearings on an NC lathe.

3. Relation between Rotational Accuracy and Processing Accuracy of Spindle

In order to ensure a high degree of roundness, surface roughness, and a high gloss surface finish of the outside diameter of a workpiece, the orbit of the shaft center (spindle axis) holding the workpiece must remain stable with every rotation. Therefore, the running accuracy (runout) of the bearing-spindle arrangement affects the geometric accuracy of a workpiece.

A spindle, however, consists of rolling bearings, housing, bearing nuts, a shaft, and many other parts. Eccentricity of the shaft orbit occurs (Fig. 1) due to manufacturing accuracy errors and assembly errors of individual parts.

The majority of components of the shaft eccentricity (displacement of the orbit of the shaft center) mentioned above are asynchronous with spindle rotation. The

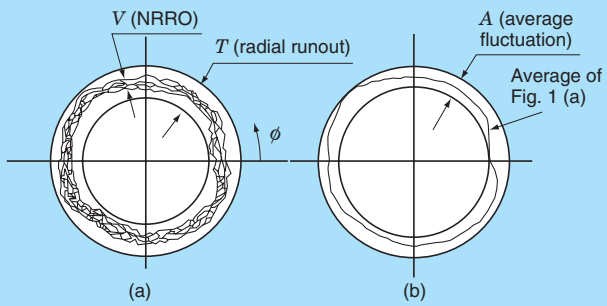

Fig. 1 Definition of running accuracy

maximum value of displacement in each phase is referred to as non-repeatable runout (NRRO), as indicated by V in Fig. 1. The average fluctuation (A in Fig. 1) is based on the average of displacement of the orbit of the shaft center for all phases during a number of spindle rotations.

An effective method for improving the precision of the machined surface geometry is to minimize NRRO and to minimize overall shaft displacement (radial runout) as indicated by T in Fig. 1.

To minimize NRRO, which greatly impacts eccentricity of the shaft orbit, we focused our attention on the precision of rollers in cylindrical roller bearings, and investigated the relation among roller accuracy, spindle rotation accuracy, and workpiece machining accuracy.

4. Evaluation of Spindle Rotation Accuracy

4.1 Spindle rotation accuracy measuring equipment

Fig. 2 illustrates the configuration of the test rig used in this evaluation. A test spindle, driven by a flat belt attached to an air driven spindle, was assembled on a test rig protected against vibrations by passive pneumatic damping.

As per ANSI/ASME B89.3.4 M-1985, a high-precision steel ball was attached to the end of the spindle as shown in Fig. 2 (a). Running accuracy was measured and calculated with the equipment configuration shown in Fig. 2 (b). At the same time, noncontact displacement transducers were set at right angles, as shown in Fig. 2 (c) and Photo 1, for obtaining Lissajous figures. Table 1 lists the rotational accuracy of the rollers that were tested. All the rollers tested under test condition A were high-precision rollers, while the rollers tested under test conditions B and C were a combination of high-precision rollers and 10 conventional precision rollers (equivalent to P5 or P4) per row, for a total of 28 rollers. (The conventional precision rollers were incorporated in the same phase location in one row of an NN3020 bearing.)

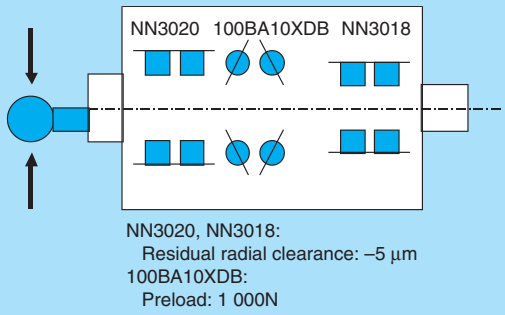

(a) Bearing arrangement on the test rig spindle

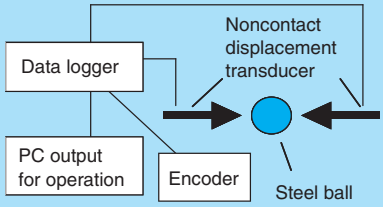

(b) Test equipment A

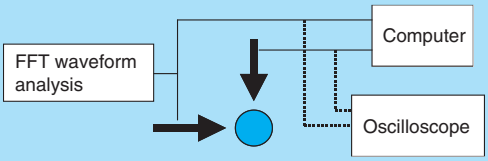

(c) Test equipment B

Fig. 2 Running accuracy test equipment

4.2 Evaluation of running accuracy

4.2.1 Radial runout of shaft center (Test equipment A)

Fig. 3 shows the results of the spindle rotation accuracy evaluation. NRRO is high throughout the entire rotation range when either the roller roundness error or the diametric difference among the rollers is large. However, the effect of roller accuracy error is small as far as the average fluctuation is concerned. This means that the errors of NRRO are reflected directly on the overall shaft displacement (radial runout) values, resulting in radial runout values that are the sums of the NRRO and the average fluctuations.

In the case of the high-precision rollers, the overall shaft displacement throughout the entire region of rotation is less than 0.3 µm. The occurrence of unstable values during testing (between 2 500 and 3 000 rpm) are due to

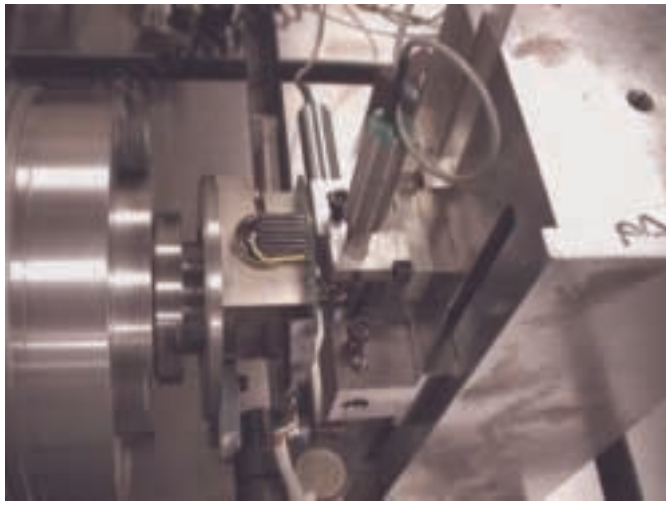

Photo 1 Lissajous figures measuring equipment

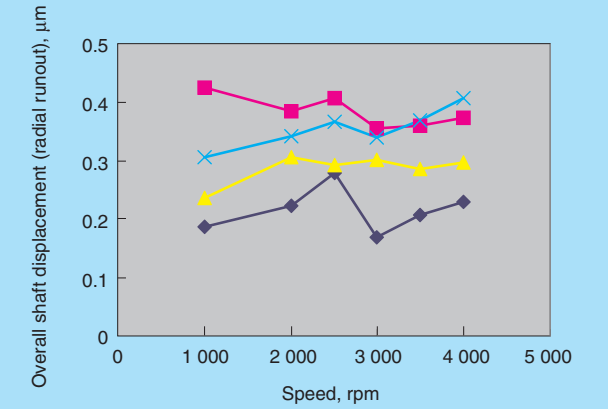

(a) Overall shaft displacement (radial runout)

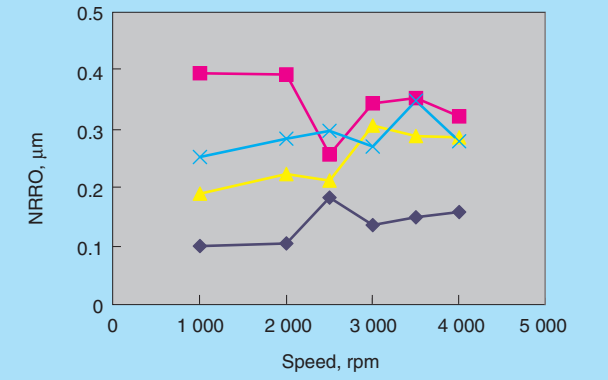

(b) NRRO

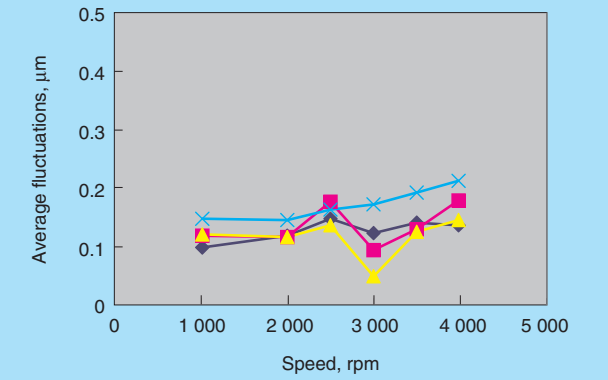

(c) Average fluctuations for an average of 8 rotations

Fig. 3 Spindle rotation accuracy test results (Test equipment A)

resonance between the natural frequency of the spindle system and certain vibration components, which are not directly associated with roller accuracy.

4.2.2 Lissajous figures (Test equipment B)

Fig. 4 shows the analysis results of Lissajous figures obtained by an oscilloscope. The wider bands indicating larger NRRO values due to larger roundness errors and larger diametric differences among the rollers can be seen. Conversely, FFT analysis of Lissajous figures (displayed as afterimages of the spindle axis loci after three to four turns of the spindle) confirms that spindle axis runout was in synchronization with the roller rotation of the spindle axis.

Table 1 Evaluation of rotational accuracy of rollers unit: µm

Accuracy of incorporated rollers	Roundness	Diametric difference among rollers
Condition A: high-precision rollers	0.1	0.2
Condition B-1: combination of rollers with large diametric variations	0.1	0.8
Condition B-2: combination of rollers with large diametric variations	0.1	0.4
Condition C: combination of rollers with large roundness errors	0.15~0.2	0.2

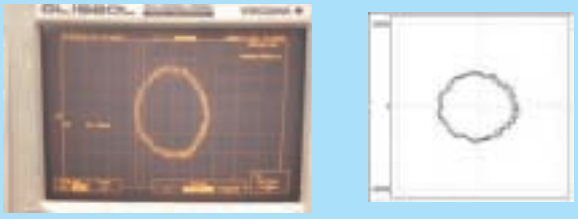

(a) Condition A: high-precision rollers

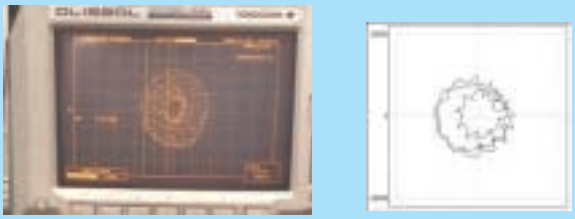

(b) Condition B-1: combination of rollers with large diametric variations

(c) Condition C: combination of rollers with large roundness errors

Fig. 4 Comparison of Lissajous figures, 1 000 rpm (Test equipment B)

5. Turning Process Test

5.1 Turning process conditions

Photo 2 shows the test rig used in this turning process test. Tables 2 (a) and (b) list the turning process conditions, and Table 2 (c) lists the accuracy of the tested rollers.

The turning conditions are equivalent to conditions for mirror finishing by a precision lathe incorporating an NSK X-Y table that feeds the cutting tool while using oil mist lubrication.

5.2 Roundness of machined surface

Fig. 5 shows the measured results for roundness of the turned surfaces. The roundness errors of the workpiece using the high-precision rollers were less than 0.3 µm (radius). Range of error variation throughout the measured surface was small, while roundness errors of the workpiece using the combined rollers (ten conventional precision rollers incorporated in the same phase location for each row of the NN3020 bearing) were as large as

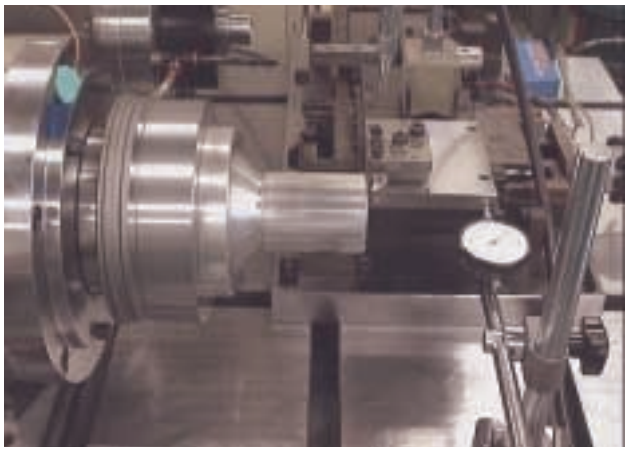

Photo 2 Turning process test machine

Table 2 Test conditions for evaluation of turned surfaces

(a) Material of work and turning process

External turning	Surface finishing to 60 mm with oil mist lubrication
Workpiece material	Al
Tool bit	Diamond with R0.6 tip
Depth of cut	0.02 mm

(b) Tool feeding

Speed, rpm	Tool feeding rate (mm/rev)
1 000	0.030
2 000	0.015
2 500	0.018
3 000	0.020
4 000	0.019

(c) Accuracy of rollers for evaluation unit: µm

Accuracy of incorporated rollers	Roundness of rollers	Diametric difference among rollers
High-precision rollers	0.1	0.2
Combined rollers	0.2	0.8

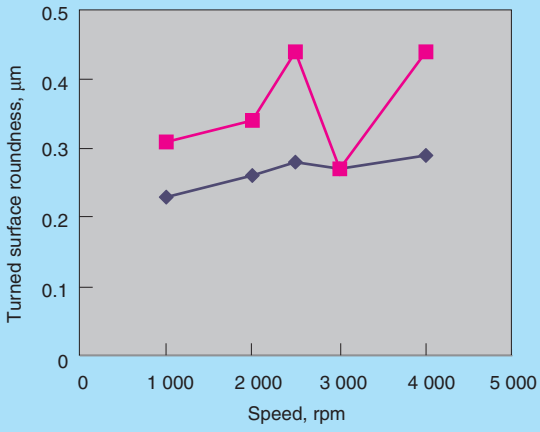

(a) Comparison of turned surface roundness (Maximum values)

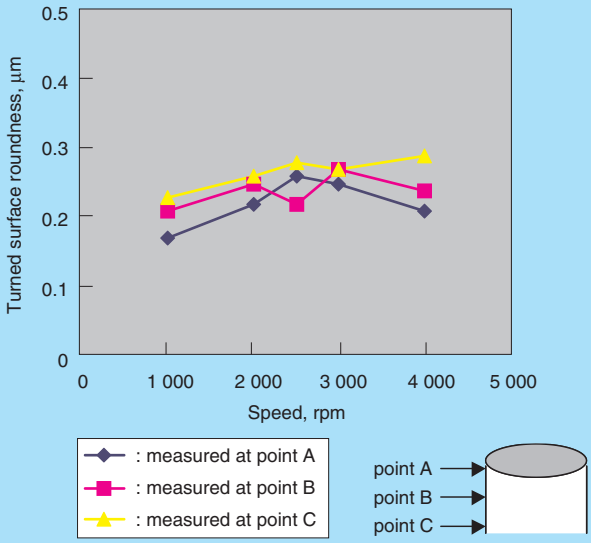

(b) Variations of roundness (High-precision rollers)

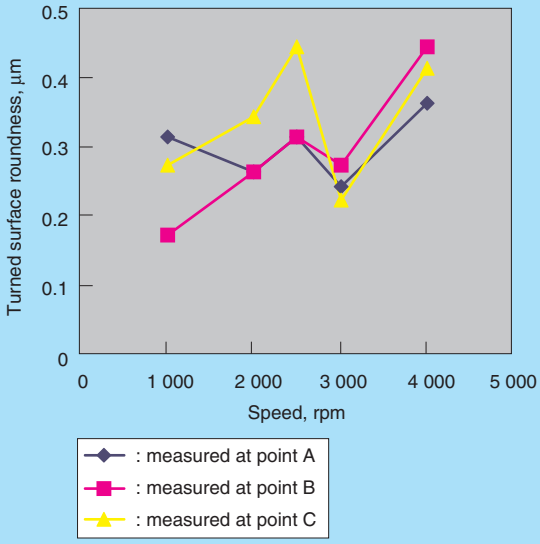

(c) Variations of roundness (Combined with conventional rollers)

Fig. 5 Roundness of turned surfaces

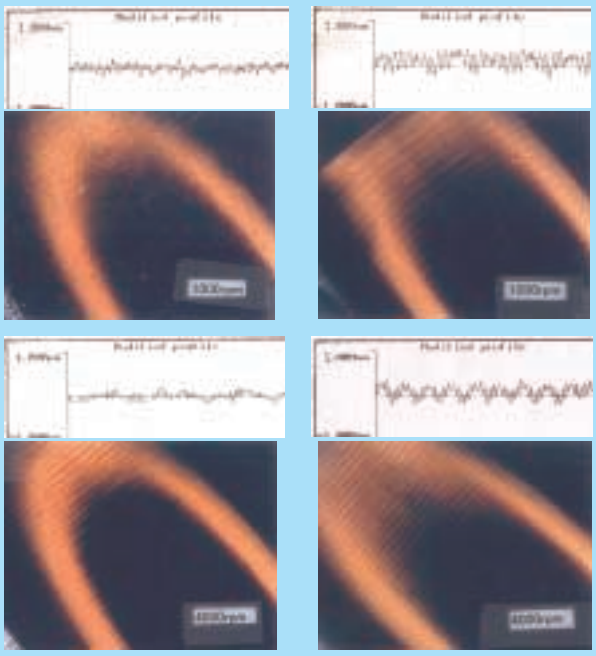

(a) High-precision rollers (b) Combined rollers

Fig. 6 Turned surface profile

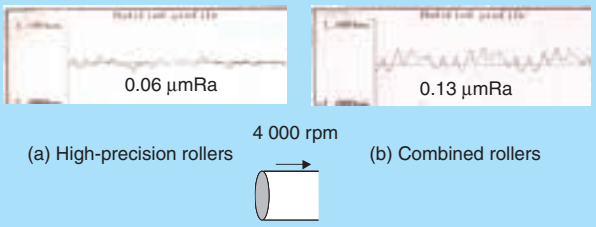

Fig. 7 Turned surface roughness

0.2 ~ 0.5 µm for both the maximum value along the axis and the overall fluctuation. When compared with the overall shaft displacement (radial runout) of the spindle, however, the difference of errors between the high-precision rollers and the combination of precision rollers and incorporated conventional rollers was insignificant.

5.3 Turned surface profiles and surface roughness

Turned surface profiles are compared in Fig. 6, and surface roughness is compared in Fig. 7. When the turning process was performed under the conditions specified in Table 2, the high-precision rollers effected little surface profile variation. The surface finish was a roughness of between 0.04 µm to 0.06 µm Ra, comparable with that obtainable by grinding and more than twice as smooth as that of the combination of high-precision rollers and conventional rollers. The surface texture produced by the combined rollers was influenced by the cycle of roller rotation of the spindle axis (component f_c).

Thus, improvements in roller accuracy to reduce component f_c can enhance the axial profile and surface roughness of the workpiece.

6. Summary

Using NSK's newly developed high-precision rollers in double-row cylindrical roller bearings for machine tool spindles used in external turning operations, we have achieved, though experimentally, a surface roundness of less than 0.3 µm. Furthermore, we achieved a machined surface roughness accuracy that is less than 0.07 µm Ra, which is almost the same level of grinding.

7. Conclusion

The machining accuracy of a machine tool depends not only on the running accuracy of its spindle, but also on various complicated factors. Such factors include the material of the workpiece, tool bits, cutting load, workpiece vibrations due to imbalance, rigidity, and dynamic imbalance of the spindle, rigidity of the tool post, and accuracy and vibration characteristics of the feed system and the control mechanism. Many recently developed NC lathes and machining centers have built-in motors where the spindle system construction is more complicated than before, thus requiring greater assembly accuracy for bearings as well as other component parts.

Provided that the machine tool is well protected against vibrations, and that the accuracy of other parts is well maintained, we believe that our newly developed super precision cylindrical roller bearings can make a significant contribution to further enhancing machine tool accuracy.

Yoshiaki Katsuno

Osamu Iwasaki

Development of the Next-Generation Half-Toroidal CVT

Takashi Imanishi and Shinji Miyata
CVT Project Team

ABSTRACT

Reducing CO_2 emissions, which cause global warming, is one of the most important challenges facing the automobile industry today. As a result, the demand for high-powered continuously variable transmissions (CVT) has been steadily increasing. The traction-drive type half-toroidal CVT meets this demand. In this paper, we will present a new concept for a three-roller system, which is compact in size and has high torque capacity, in addition to a power-split system that has extremely high efficient capability.

1. Introduction

NSK started research and development of traction-drive type toroidal continuously variable transmissions (CVTs) in 1978. The successful outcome of our research and development was first installed in the Nissan Cedric and Nissan Gloria sedans, which were introduced into the market in November 1999. The toroidal CVT, an idea that was born in a U.S. patent[1] in 1877 by Charles Hunt, was practically embodied as an automotive transmission after a lapse of more than one hundred years. There were many years of difficulties and challenges that had to be overcome before building a toroidal transmission having practical and serviceable endurance in a size and torque capacity suitable for automotive applications. The concept of a half-toroidal transmission, featuring a contact angle maintained at the power rollers for reducing spin loss of the traction power transmission, is what opened the door to a high-power toroidal CVT. This design permits an increase in transmission power at each contact point. In addition, Machida et al. succeeded in further downsizing and increasing power augmentation by applying longer bearing life technology to the power rollers of the toroidal CVT[2]. Fig. 1 shows the chronology of torque capacities of half-toroidal CVTs. We can see that half-toroidal CVTs, whose developments were initiated in the 1960s, began with a torque capacity that sharply increased. This lead to promising commercialization of CVTs after 1990, when longer bearing life technology was applied to the power rollers.

With the continually increasing global concern for energy conservation, users demand a toroidal CVT that is compact and has greater efficiency and higher torque capacity. Automobiles currently available on the market that are equipped with a half-toroidal CVT have already achieved a 10 percent improvement in fuel economy under the Japanese Ministry of Transport mixed cycle (10-15 mode) test. Regardless of this achievement, the never-

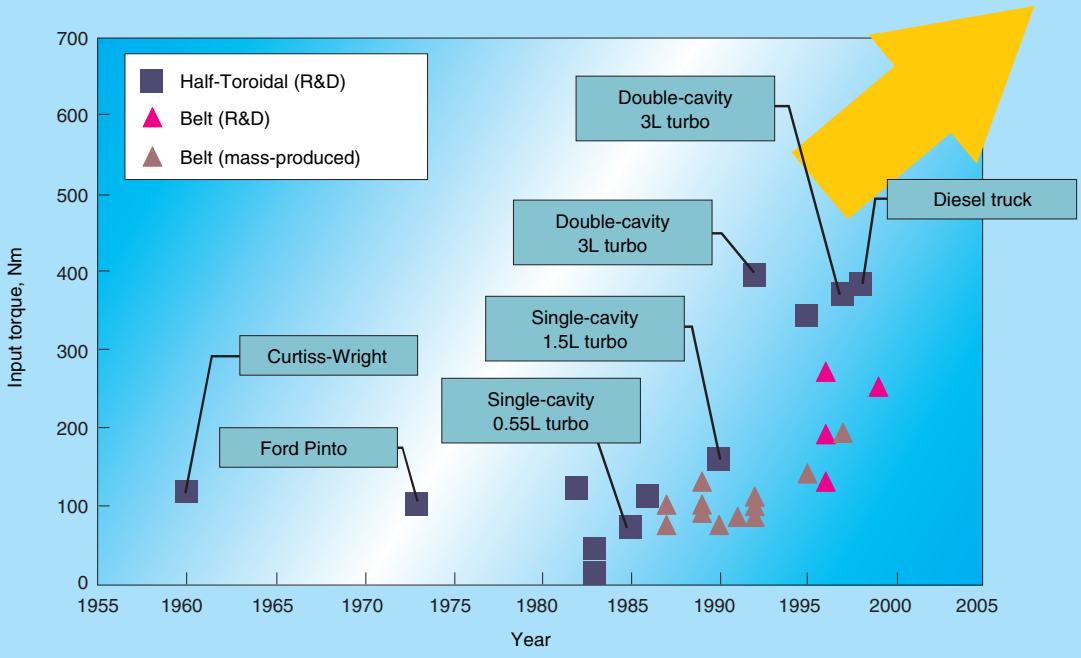

Fig. 1 Progress of the half-toroidal CVT

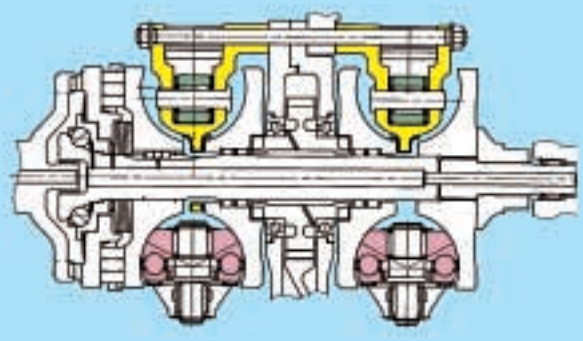

Fig. 2 Three-roller half-toroidal CVT

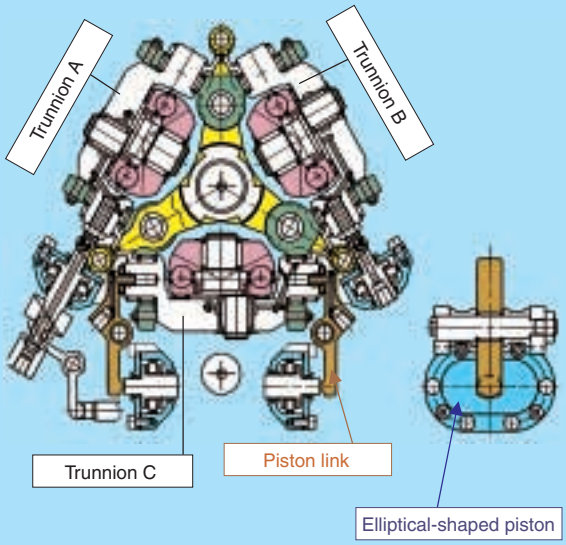

Fig. 3 Three-roller half-toroidal CVT

ending demand for even greater fuel economy requires even better CVTs with higher efficiency. We are reporting here on a power-split system that can achieve such higher efficiency and a wider range in speed ratio by combining continuously variable toroidal reduction gears and planetary gears with a three-roller CVT in a size and capacity that is compatible with large passenger vehicles.

2. Three-Roller CVT

In a traction drive system, the tangential force at the point of power transmission is expressed as:

$$Ft = n \cdot \mu \cdot Fc \quad \ldots\ldots\ldots\ldots\ldots\ldots\ldots\ldots\ldots\ldots (1)$$

where an increase in Ft leads to higher torque capacity and a reduction in size. As can be seen in Equation (1), Ft can be increased by increasing n, μ, and Fc, respectively.

Whereas μ depends on the characteristics of traction oil, the development of new oils in the future is expected to contribute significantly to greater torque capacity. An increase of Fc mainly affects the rolling fatigue life of material, as seen by the actual application of longer bearing life technology, which enhances the service life of the traction drive as mentioned earlier. An increase of n means an increase in the number of power rollers for increased torque capacity and greater reduction in size. NSK's three-roller system, as reported here, has a torque transmission 1.5 times greater than that of our conventional two-roller system. Alternatively, if there is no need to increase torque capacity, then the three-roller system can be used for achieving greater size reductions accordingly. Figs. 2 and 3 show cross-section views of NSK's newly developed three-roller CVT, with specifications listed in Table 1. In a toroidal CVT, it is necessary to attach a hydraulic piston for ratio control to each of the three trunnions. However, for a three-roller system where three trunnion shafts intersect each other, it is difficult to arrange hydraulic pistons in the limited space of the transmission housing. For this reason, the hydraulic pistons of our newly developed three-roller system are setup in a unique arrangement. Trunnions A and B are each fitted with a double-acting piston. Trunnion C, however, is fitted with a single-acting piston, whose generated force is transferred to the trunnion by a link mechanism. Additionally, in order to reduce the size of the pistons along the minor axis perpendicular to the main shaft (Fig. 3), the pistons are designed with a cross-sectional profile in the shape of an elongated circle (ellipse) whose major axis is parallel to the main shaft. The single-acting piston attached to trunnion C shares the same elliptical-shaped cross profile, but has a simpler design since there is need to rotate around its axis. A double-acting piston is attached to trunnion A and another to trunnion B. Since both pistons must be able to rotate when tilted, a thrust bearing is interposed between the respective piston and the shaft so that the shaft can rotate smoothly whenever load is applied to the piston.

This high-power, compact, three-roller system can thus satisfy greater torque requirements for large-sized luxury vehicles.

Table 1 Specification of three-roller CVT

Cavity diameter, D [mm]	120
Disk radius, r_o [mm]	36.5
Half value of contact angle of power roller, θ_o [deg]	62.5
Number of power rollers, n	3
Inclination angle of rotating power roller, ϕ [deg]	27.5~97.5
Variator reduction ratio, i_{CVT}	2.344~0.427
Variator ratio range	5.49
Maximum input torque, T_{max} [Nm]	430
Maximum input speed, N_{max} [rpm]	6 000

3. Power-Split System

3.1 Theoretical transmission efficiency of power-split system

As far as we know, Okoshi invented the first power-split system in 1987[3]. Okoshi's invention requires two sets of planetary gears and involves a complicated construction. The authors therefore conceived a new system layout that features one set of planetary gears in a simpler construction (Fig. 4).

This system is composed of the three modes: low-speed mode, high-speed mode, and reverse mode. In the low-speed mode, engaging the low-speed clutch (K1) and shifting the variator for acceleration results in high-speed output. In the high-speed mode, engaging the high-speed clutch (K2) for deceleration results in output rotation from the sun gear as a differential component of the carrier and the ring gear.

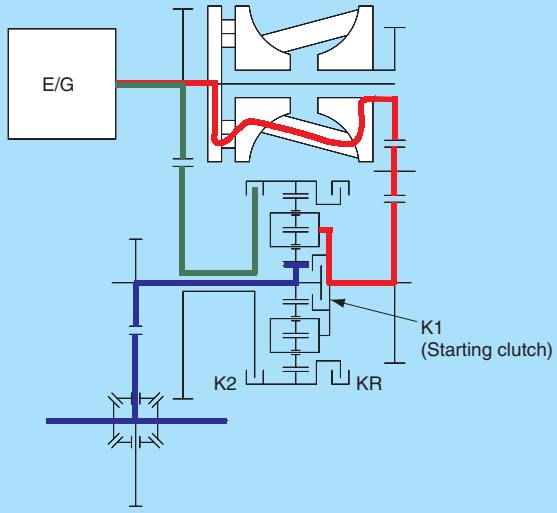

Fig.4 Layout of power-split system for FF vehicles

Using Morozumi's formula for transmission efficiency, ηo, of planetary gears[4], and the theoretical formula of Machida et al. for efficiency of transmission from the variator[5], theoretical efficiency of power transmission from the engine shaft to the sun gear in Fig. 4 can be expressed as:

$$\eta_{total} = \frac{\eta_0 (i_0 i_1 i_2 i_v + 1 - i_0)}{i_0 i_1 i_2 i_v + \eta_v \eta_1 \eta_2 (\eta_0 - i_0)} \quad \cdots\cdots\cdots\cdots\cdots\cdots (2)$$

3.2 Power-split system verification by experiment

Experimentally, we measured the power and the transmission efficiency of the power-split system having a single-cavity CVT (See Table 2). A layout of the power-split system is illustrated in Fig. 5. We used a 300 kW DC power absorption dynamometer to determine the amount of power passing through the power-split system. Torque and the number of rotations were measured ① at system output, ② between the variator output shaft and the planetary gear system, and ③ at the bypass shaft. Engaging and disengaging the coupling performed switching between low-speed and high-speed modes.

Fig. 6 shows speed variation test results of the power-split system operated at a constant speed under no load. We can see that the output speed continuously varies in proportion to the variation ratio of the variator. The measurements and the theoretical lines agree with each other in Fig. 6. Fig. 7 shows the power measured at the three points as specified earlier. This figure illustrates that power, approximately 1.7 times as high as the power to the power-split system, passed through the bypass

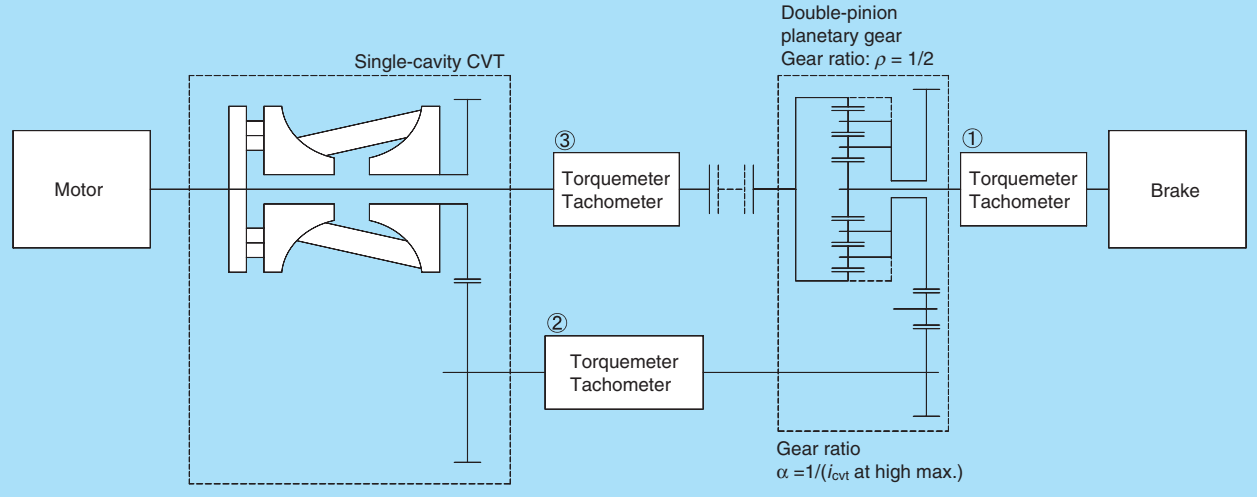

Fig. 5 Layout of power-split system for bench test

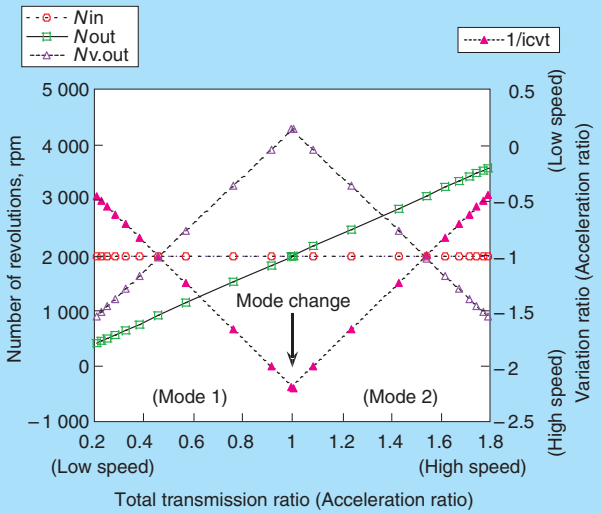

Fig. 6 Results of test under no load

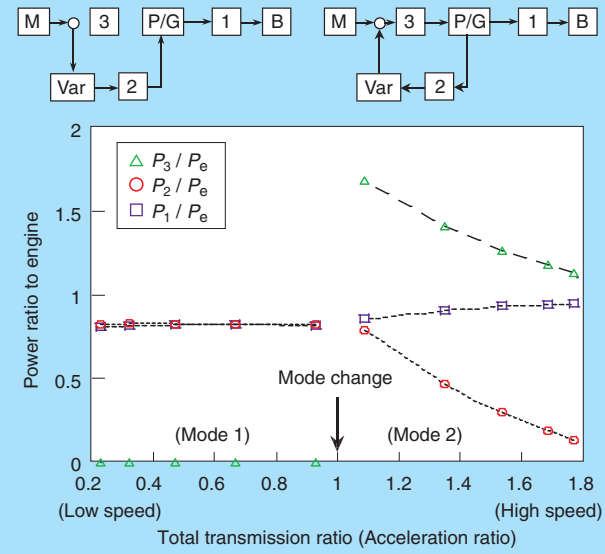

Fig. 7 Results of power measurement of power-split system

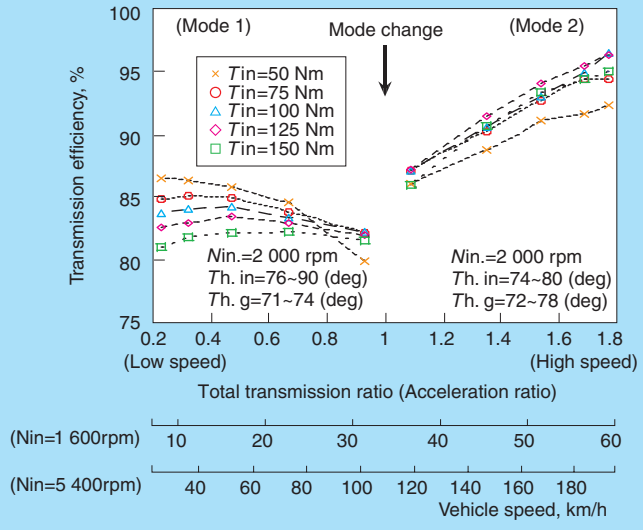

Fig. 8 Efficiency of power-split system

Table 2 Specification of single-cavity variator

Maximum input torque, [Nm]	150
Total transmission ratio width	8.6
Variator ratio	4.8
Outer diameter of disk, [mm]	156
Cavity diameter, D [mm]	132
Disk radius, r_o [mm]	40
Half value of contact angle of power roller, θ_o (deg)	62.5

shaft3) immediately after the mode change. In high-speed mode, power flowing through the variator declines proportionately with the variation ratio, which, in the final stage, corresponds to the highest speed of an actual car with only 10 percent of the power to the power-split system flowing through the variator. Furthermore, in high-speed mode, power passed from the output disk side to the input disk side, which matches the theoretical lines indicated in Fig. 7. Fig. 8 shows the measurements of transmission efficiency for this power-split system. The axis of abscissa represents the variation ratio of the power-split system and car speeds at engine speeds of 1 600 rpm and 5 400 rpm. Transmission efficiency of the entire system was 80 to 85% in the low-speed mode, but achieved a maximum of 96% in the high-speed mode.

The results discussed here pertain to a power-split system containing a single-cavity CVT designed for a small front engine, front-wheel drive (FF) vehicle. Additionally, this CVT is compact and consists of a relatively few number of parts. It is also possible to apply the same power-split system to a double-cavity CVT. For a double-cavity CVT incorporating a power-split system, theoretical transmission efficiency is approximately 90% in the low-speed mode, and its maximum theoretical transmission efficiency is expected to be 97%, as shown in Fig. 9.

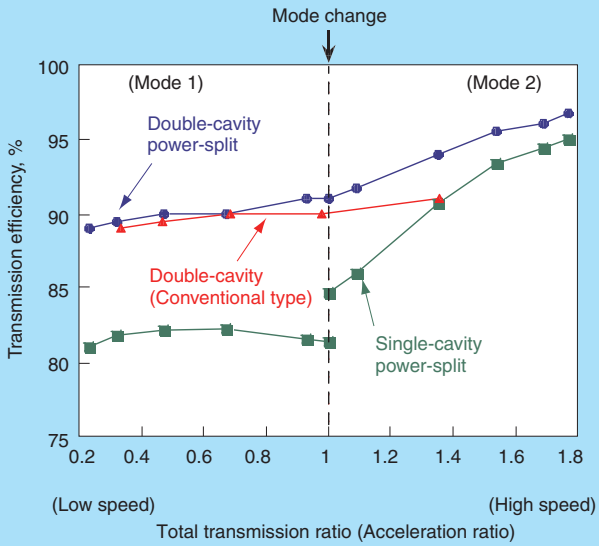

Fig. 9 Theoretical efficiency of double-cavity power-split system

Photo 1 Three-roller power-split CVT

4. Conclusion

Photo 1 shows a model of the three-roller power-split system that went on display at the 2001 Tokyo Motor Show. This model is of the next-generation half-toroidal CVT developed by incorporating the two technologies described in this report. As CVT technology becomes more prevalent in the future, we anticipate making an even greater impact on protecting the environment. We will continue to challenge ourselves in making further developments for a three-roller power-split CVT system that will achieve greater reductions in size, deliver higher output, and boost fuel economy.

References:

1) USP 197, 472.
2) H. Machida and T. Abe, "Fatigue Life Analysis of A Traction Drive CVT," JSAE Proc. of CVT' 96, 9636402 (1969) 6P.
3) Japanese patent No. 2929592.
4) M. Morozumi, "Engineering Calculation Method for Planetary Gear and Differential Gear," Sankei Shuppan.
5) H. Machida, H. Itoh, T. Imanishi, and H. Tanaka, "Design Principle of High-Power Traction Drive CVT," SAE Paper 950675 (1995) 11P.

Takashi Imanishi

Shinji Miyata

Development of Wedge Roller Traction Drive Units

Hiroyuki Ito, Satoshi Dairokuno, and Hideo Okano
Corporate Research and Development Center

ABSTRACT

Our Wedge Roller traction drive unit utilizes a traction drive for attaining excellent features such as high efficiency, and quiet, smooth power transmission by configuring the traction drive transmission to a motor. In this paper, characteristics of our newly developed Wedge Roller traction drive unit are reported.

1. Introduction

Power transmissions that incorporate a traction drive, which is capable of quiet and smooth operations with minimum vibration, have been in the limelight in recent years. In 1999, NSK succeeded in the commercialization of a half-toroidal CVT for 3L turbo vehicles[1]. A traction drive transmits power by the shear force of the elastohydrodynamic lubrication (EHL) oil film that is formed under a large contact force, which is generated in the power transmission system. However, industrial machinery, automotive actuators, and auxiliary equipment have been gradually changing from hydraulic drives to electric drives for energy saving benefits and because of the prevalence of sophisticated electronic controls. In 1998, NSK developed a Wedge Roller traction drive unit for electrical power-assisted bicycles[2], which only consisted of the reduction unit. In anticipation of increased applications that make use of high-speed motors combined with a reduction unit, NSK developed a new Wedge Roller traction drive unit that is compact and incorporates a motor assembly with the reduction unit.

2. Mechanical Description

2.1 General description

Fig. 1 shows a cross section view of the Wedge Roller traction drive unit, in which the reduction unit is on the left, and the motor assembly is on the right.

Power is generated in the brushless motor by a stator and rotor, and transmitted through the motor shaft, which is coupled to the input shaft of the reduction unit. Torque is transmitted from the input shaft through three rollers to the inside surface of the output ring. Slots are available near the edge of the output ring. The reduced torque is transmitted to the output shaft that fits in the slots.

Fig. 2 illustrates the structure and function of the reduction unit mechanism. The input shaft and output ring are parallel to each other, but slightly offset (eccentric). One of the three rollers is slightly larger in diameter than the other two, and one of the two small rollers is movable with a wedge angle (wedge roller). All three rollers fit in the space between the output ring and the input shaft. Two of the rollers, the large one and one small one, are fixed by bearings, and can rotate on their own axes.

When the input shaft rotates counterclockwise, the wedge roller moves in the direction of the wedge in proportion to the transmitted torque. Contact force is extended to the guide rollers through the input shaft and the inside surface of the output ring. Since the wedge roller moves in the direction of the wedge, adequate contact force in proportion to the torque is constantly generated. Therefore, transmission efficiency is high, even when the torque is low.

The wedge roller moves in the direction of the wedge when input torque is generated, and the output ring, which contacts the rollers, is also moved slightly. This construction allows free movement of the output ring in the radial direction.

However, when torque is transmitted from the output ring, the wedge roller moves away from the wedge. This mechanism prevents power from being transmitted, leaving the wedge roller idle, and thus never driving the motor in reverse.

The placement of the housing between the motor and the reduction gear makes it possible to support the input shaft

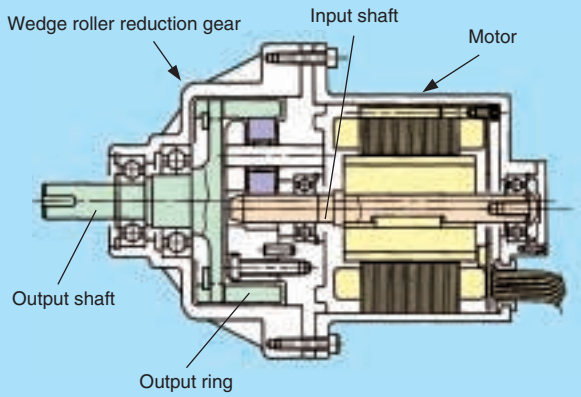

Fig. 1 Wedge Roller traction drive unit

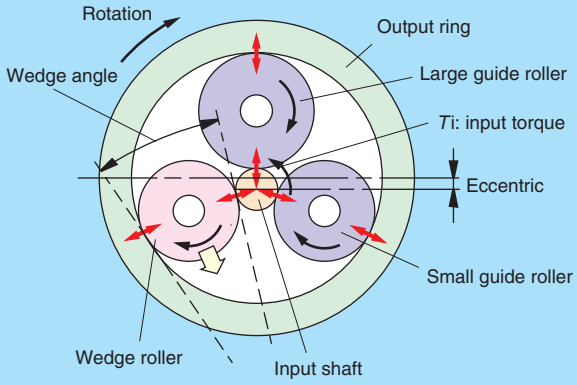

Fig. 2 Structure and function

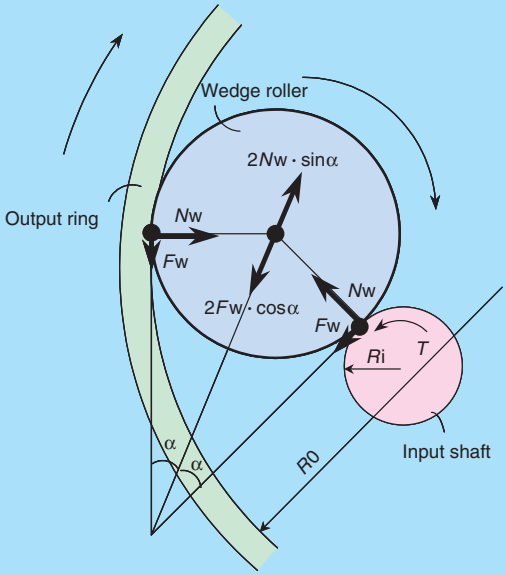

Fig. 3 Mechanism of contact force generation

retaining bearing and the guide roller holding pins. The housing also acts to separate and protect the motor from lubricant contamination.

Spring loaded pins move the wedge roller in the direction of the wedge in order to provide contact force for preloading.

2.2 Principle of contact force

Fig. 3 shows torque T from the input shaft being transmitted to the output ring by traction drive. The wedge roller moves in the direction of the wedge (wedge angle 2α) between the input shaft and the output ring. The input shaft and output ring then come in contact with the guide rollers. Fw represents the tangential force transmitted from the input shaft and the output ring to the wedge roller. Nw represents the normal force that is thus simultaneously generated. When we consider the balance of the force being applied in the direction of the wedge, a contact force proportionate to the torque is constantly generated because:

$$2F\mathrm{w}\cdot\cos\alpha = 2N\mathrm{w}\cdot\sin\alpha$$

$$\therefore F\mathrm{w} = N\mathrm{w}\cdot\tan\alpha$$

The generated traction force Ft is given as

$$F\mathrm{t} = \mu\cdot N\mathrm{w}$$

μ : traction coefficient

In order for the power to be transmitted without gross slippage, the follow must be true:

$$F\mathrm{t} \geq F\mathrm{w}$$

$$\therefore \alpha \leq \tan^{-1}\mu$$

2.3 Reduction ratio

The reduction ratio, λ, is a ratio of the output ring and the input shaft diameters:

$$\lambda = R\mathrm{o}/R\mathrm{i}$$

2.4 Lubricant

Any lubricant used in the traction drive unit must have a high traction coefficient. The lubricant used in this Wedge Roller traction drive unit is either traction oil used in half-toroidal CVTs, or traction grease that has similar characteristics to traction oil[3].

3. Performance Measurements

Photo 1 shows two Wedge Roller traction drive units we built to evaluate performance. Specifications for both units are listed in Table 1. Evaluation results of the motor for the smaller traction drive unit (250W) are shown in Fig. 4. Testing under practical operating conditions revealed an efficiency of 80 to 85 percent. The efficiency of the reduction unit only was also evaluated[4].

Efficiency of the larger traction drive unit (1kW) is shown in Fig. 5. Efficiency exceeded 90% in the low-torque

Photo 1 Wedge Roller traction drive units

Table 1 Specifications of Wedge Roller traction drive units

	Reduction gear motor 1	Reduction gear motor 2
Rated motor output power	250 W	1 kW
Rated output speed	600 rpm	600 rpm
Rated output torque	4 N·m	16 N·m
Input shaft diameter of reduction unit	ø8 mm	ø12 mm
Reduction ratio	6.0	6.0
Lubricant	Grease	Oil

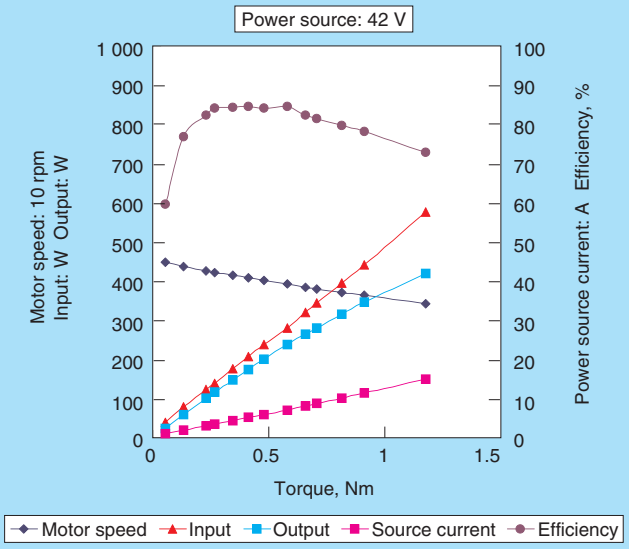

Fig. 4 Drive unit with 250 W motor

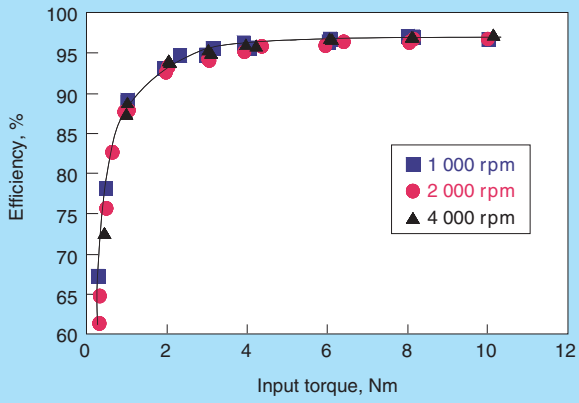

Fig. 5 Power transmission efficiency of drive unit

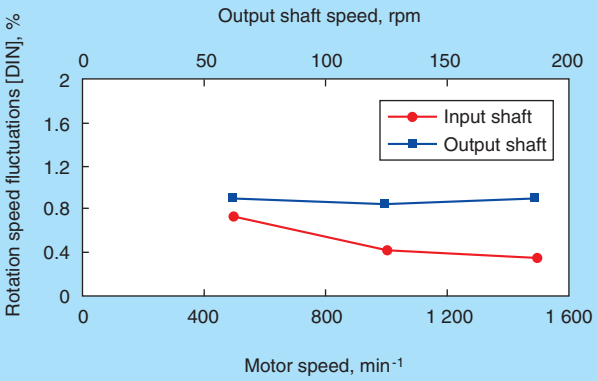

Fig. 6 Fluctuation of drive unit

range and reached a maximum of approximately 97%. This indicates that output torque of the motor can be transmitted with very little loss of efficiency. Motor speed seems to have very little effect on efficiency, as well. Although not shown here, evaluations were also made for traction oil and traction grease. Both lubricants performed equally well with no marked difference in efficiency. Speed fluctuations of the traction drive unit were measured and reported in Fig. 6. Fluctuations decreased as speed was increased.

4. Prospects for Future

Although the above description is focused on the Wedge Roller traction drive unit consisting of a motor-driven reduction unit, we can also consider usage of this unit as a generator when power is applied from the opposite side (output shaft). It is also possible to transmit power in both directions by converting the small guide roller into a wedge roller, and by applying force to both of them. By preloading each wedge roller with a spring, and by controlling the positions of the supporting pins, the drive unit can be used for various applications. In addition, the traction drive unit can be further developed to make use of its low-noise and low-vibration features for use in high-speed rotation applications.

The traction drive unit has thus far been developed as a unit for small motors. For applications in industrial machinery and automobiles, however, medium or high power units need to be further developed.

In a unit having larger capacity, the motor will naturally be hotter, and the traction drive mechanism adjacent to it will require greater resistance to higher temperatures. Such a unit will have to be designed for better heat radiation efficiency, and will require development of a lubricant applicable to higher temperatures. Developments in geometric design, materials, and heat treatment are very important to design a unit with higher torque capacity over 10kN normal force at the power transmission point.

References:

1) H. Machida and Y. Murakami, “Development of Traction Drive CVT POWERTOROS Unit—Report No. 1,” NSK Technical Journal No. 669 (2000) 9-20.
2) R. Otaki, K. Sakai, and H. Machida, “Wedge Roller Traction Drive Transmission,” Collection (VI) of Lecture Texts at 75th General Meetings of Japan Society of Mechanical Engineers, No. 98-1 (1998) 223-224.
3) M. Yamanaka, Y. Yamazaki, K. Inoue, and H. Hata, “Evaluation of Characteristics of Traction Grease at Low Temperature,” MPT2001-Fukuoka, The JSME International Conference on Motion and Power Transmissions, 1 (2001) 826-831.
4) R. Otaki and H. Machida, “Study of Traction Drive Transmission Using Wedge Action,” MPT2001-Fukuoka The JSME International Conference on Motion and Power Transmissions, 1 (2001) 832-837.

Hiroyuki Ito

Satoshi Dairokuno

Hideo Okano

High Straightness Positioning Stage Implementing Real-time Position Compensation

Akihisa Amada and Michio Tsunoda, Technology Development Division-Headquarters
Osamu Kanasashi and Katsuyoshi Imai, NSK Precision Co.,Ltd.

ABSTRACT

With the ongoing trend of miniaturization of the semiconductor manufacturing process, better velocity stability and straightness of travel are required for stages used in semiconductor equipment such as an exposure machine and defect inspection machine.

In this article, we will introduce NSK's newly developed stage, which achieves exceptional straightness of travel while incorporating a non-contact stage and fine motion stage with real-time error compensation. Our new stage meets the needs and requirements of the semiconductor manufacturing and processing market.

1. Introduction

The growing trend towards even greater miniaturization of semiconductor fabrication requires the use of extremely accurate *XY* positioning stages for exposure equipment, defect inspection devices, and more. Initially, point-to-point positioning, motion to target position from a current position, was common to the *XY* positioning stages for these applications. Nowadays, scanning that conducts exposing or inspecting operation during the table motion is adopted in order to increase process throughput. (Scanning: In a two axes *XY* positioning stage, one axis table performs a motion at a constant speed, i.e. scanning, while the other axis table is performing a step motion.) For this reason, operations of positioning stages must be at a constant speed with exceptional straightness of travel. To meet such requirements, NSK has developed an *XY* positioning stage that achieves exceptional straightness of travel by incorporating a fine-motion table capable of real-time position error compensation.

2. Stage Construction and Specifications

NSK's newly developed *XY* positioning stage is shown in Fig. 1, and its schematic diagram is shown in Fig. 2. It consists of a coarse-positioning *Y*-axis base table, which is equipped with linear guides and driven by a ball screw, an *X*-axis table, which is equipped with pneumatic linear bearings and driven by a linear motor, sitting on the *Y* axis base table, and, at the very top of the stage, an electromagnetically actuated fine-motion *Y*-axis table with leaf springs, a *Z*-axis, and a θ–axis.

The purpose of this table is to ensure high travel straightness of the *X*-axis table by the constant position compensation in the direction of the *Y*-axis while the *X*-axis table is traveling at a constant speed. When the *X*-axis table travels at a constant speed, the *Y*-axis table compensates for any deviation error on the *X*-axis, thus constantly maintaining the *X*-axis table in an accurate position.

This requires a *Y*-axis table that is capable of working accurately at high speeds. This is achieved by combining

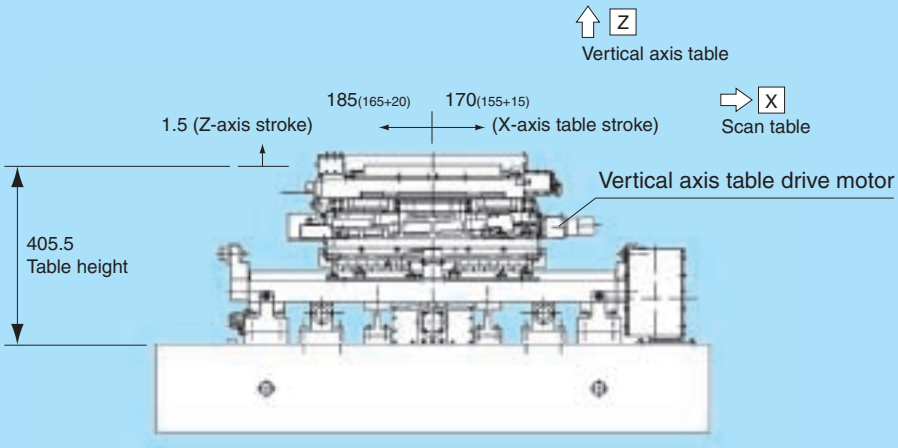

Fig. 1 *XY* positioning stage

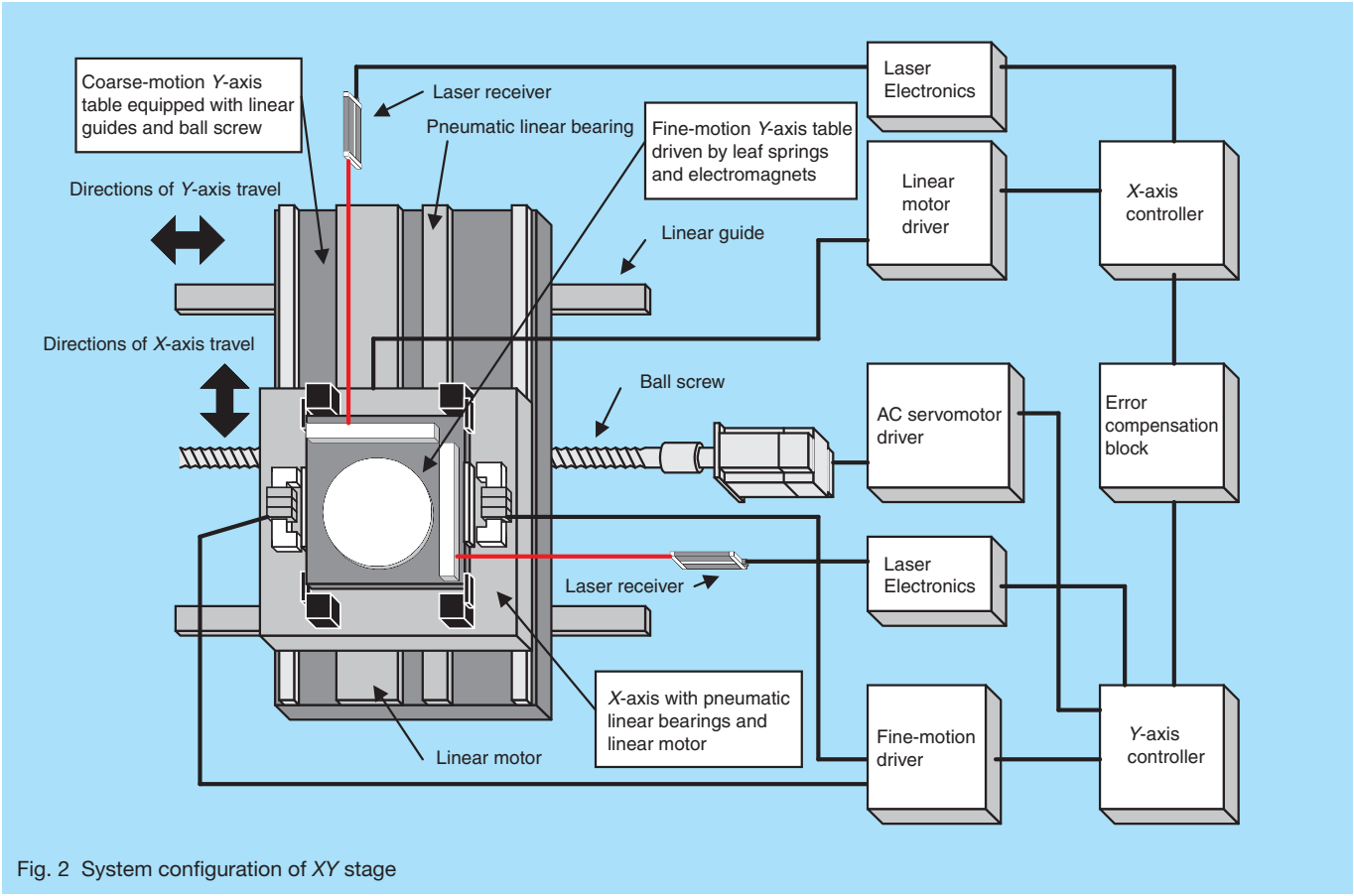

Fig. 2 System configuration of *XY* stage

Table 1 Specifications of *XY* stage

Axis	Item	Value
X	Stroke	300 mm
	Maximum speed	250 mm/s
	Repetitive positioning	±0.1 μm
	Speed stability (at 50 mm/s)	±1% or less
	Straightness (at 20 mm/s)	Without compensation ±1.0 μm
		With compensation ±0.015 μm
Y	Stroke	300 mm
	Maximum speed	250 mm/s
	Repeatability	0.015 μm

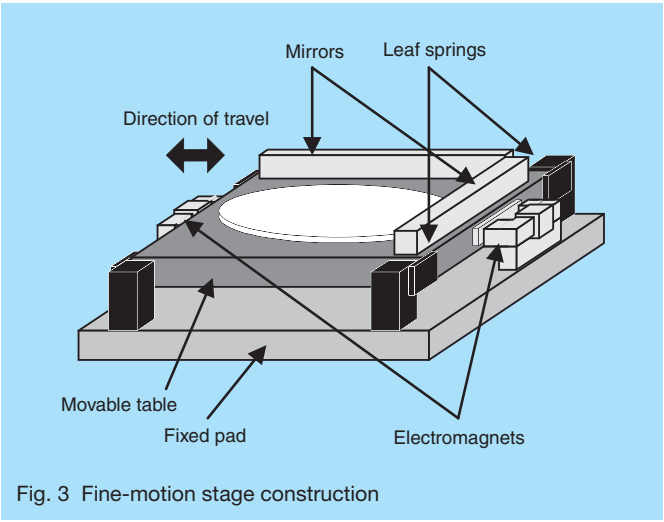

Fig. 3 Fine-motion stage construction

the electromagnetically actuated fine-motion *Y*-axis table with the coarse-positioning *Y*-axis table. Specifications of this *XY* positioning stage are listed in Table 1.

3. Construction of Fine-Motion Y-axis Table and Motion Compensation

3.1 Fine-motion *XY* stage construction

Fig. 3 shows the fine-motion *Y*-axis table, which is secured by leaf springs to the center of the base. Motion is controlled by electromagnets located on both sides of the base. This construction is frictionless, thus allowing the fine-motion *Y*-axis table to move quickly with greater accuracy.

3.2 Motion compensation

Laser measuring systems are used to monitor positions of the *X*-axis and the *Y*-axis tables (Fig. 4). The amount of travel and position of the tables are controlled by the monitored position data. The *Y*-axis table consists of the coarse-motion base axis table and the fine-motion axis table, whose positions are detected by one laser measuring system so that the control of both axes is switched

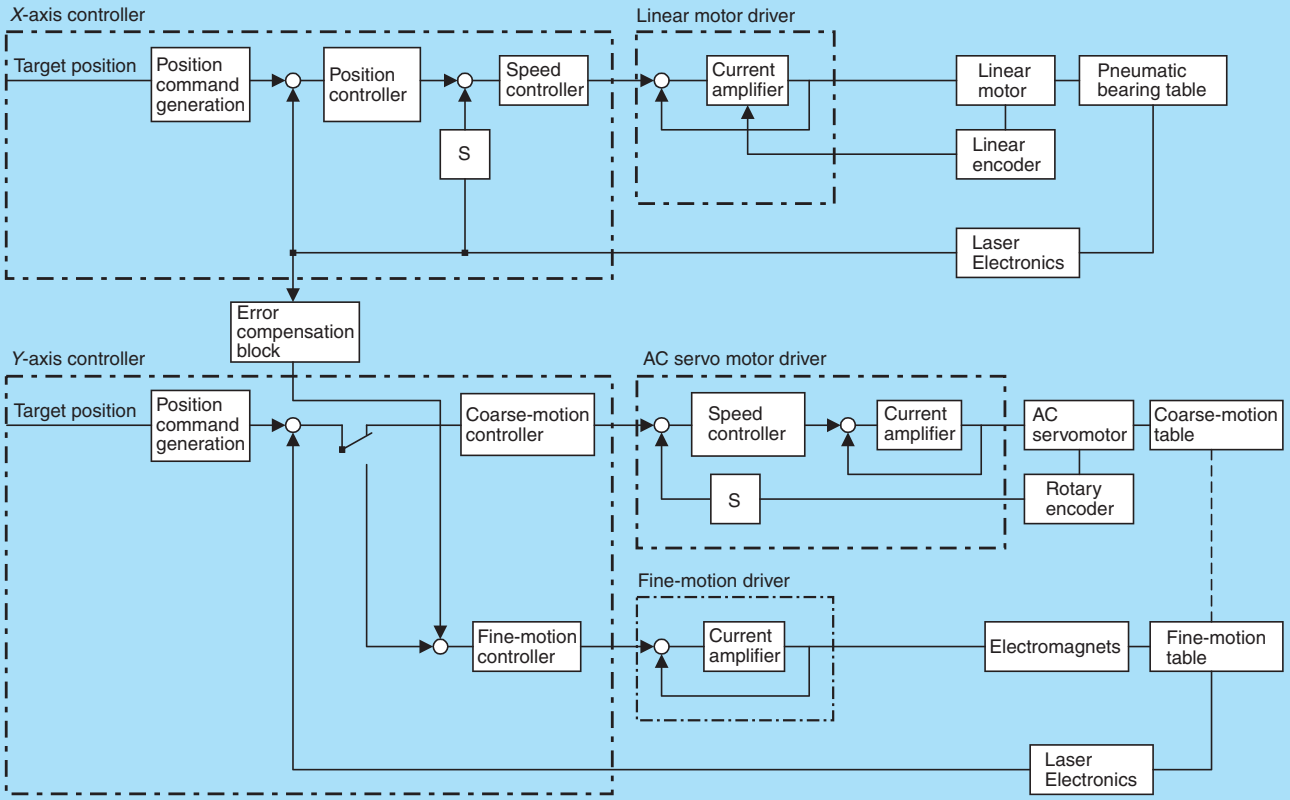

Fig. 4 *XY*-axes control block diagram

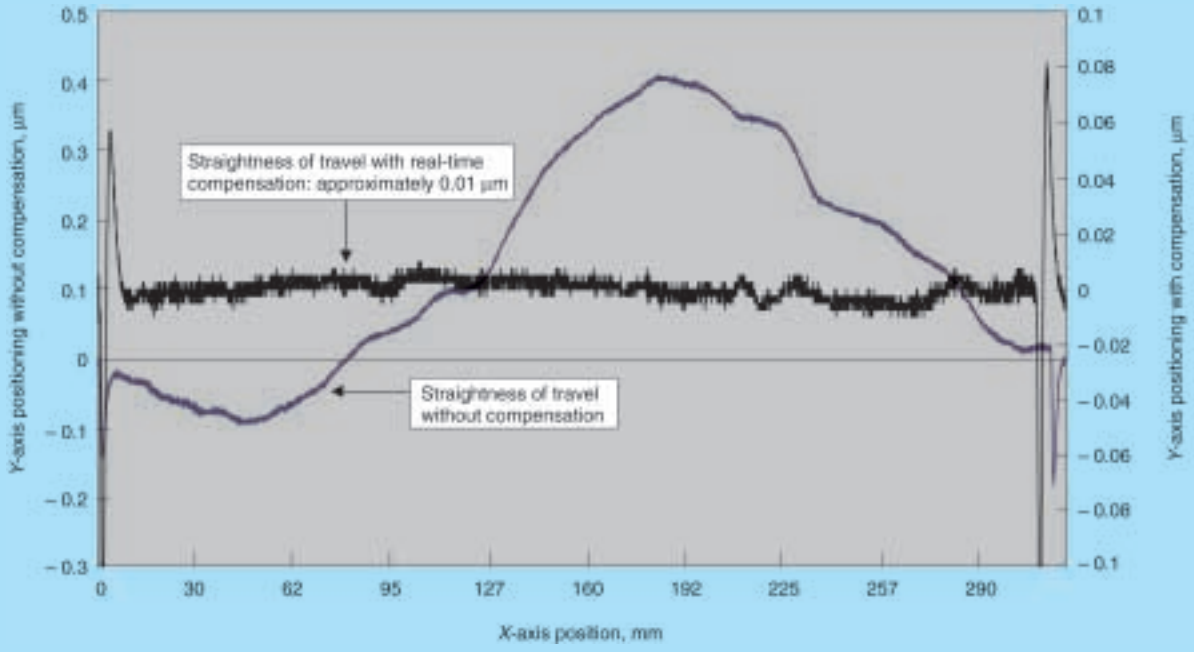

Fig. 5 Straightness of *X*-axis travel with and without compensation

according to the distance to the target position.

To compensate for straightness of the *X*-axis positioning table, position information from the laser measuring system for the *X*-axis positioning table is sent to the error compensation block, whose outputs control the fine-motion *Y*-axis table. With these measures, the fine-motion *Y*-axis table can repeat real-time compensations while the *X*-axis table is traveling. Thus, the *XY* stage performs with highly

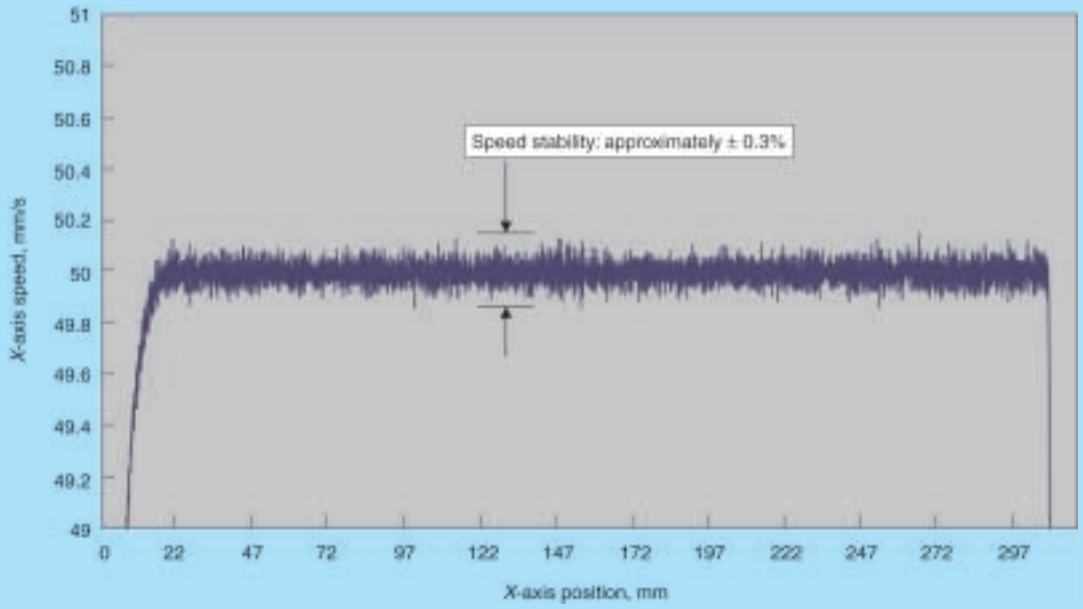

Fig. 6 Stability of *X*-axis velocity

precise straightness of travel.

The amounts of compensation corresponding to the positions of the *X*-axis table need to be stored in advance in the error compensation block. The positioning repeatability of the *XY* stage is also important. In order to assure excellent repeatability of the *X*-axis table, a frictionless pneumatic linear bearing and a non-contact linear motor are used.

4. Results of Motion Compensation

Fig. 5 illustrates the straightness of travel of the *X*-axis table with and without compensation. As shown in the figure, a 300 mm stroke without compensation results in the straightness of travel of 0.5 µm, while with real-time compensation, it is reduced to about 0.01 µm. Furthermore, velocity of the *X*-axis table remains fairly constant, with a minimal amount of fluctuation at about ± 0.3%.

5. Conclusion

Our XY positioning stage configuration, which includes an electromagnetically actuated fine-motion table and non-contact pneumatic linear bearings with high repeatability, has resulted in an *XY* stage with excellent straightness of travel.

Whereas the current mechanical accuracies of *XY* positioning stages have nearly reached their limit, we feel that NSK's real-time compensation system will significantly benefit various applications.


Akihisa Amada


Michio Tsunoda


Osamu Kanasashi


Katsuyoshi Imai

High-Rigidity Type Monocarrier®

The Monocarrier® is a compact actuator in which a ball screw is integrated with a linear guide. In addition to many other features, the NSK Monocarrier® is compact, easy to install, and provides customers with long term, maintenance-free performance. The Monocarrier® has been widely used in the FA field because of its "ease-of-use."

Recently, the new Monocarrier®, that is, MCH type (Photo 1) having higher rigidity as a beam than conventional types and a lightened model MCL06, which has lower rail height than MCH06, have become available. We introduce this type as follows:

1. Outline of MCH/MCL Types

Cross sections of the newly developed Monocarrier® are shown in Fig.1. Three high-rigidity models (MCH06 [60 mm rail width], MCH09 [86 mm rail width] and MCH10 [100 mm rail width]), and MCL06 that features a lighter rail have been added.

Photo 1 Monocarrier® MCH Type

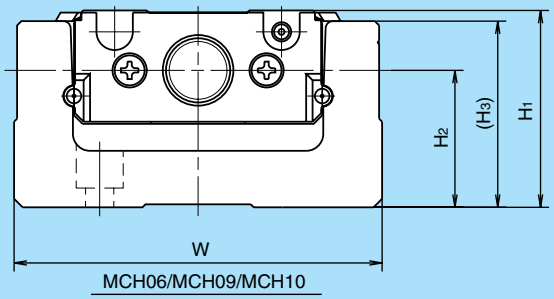

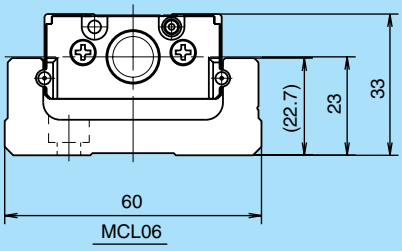

Model No.	W	H_1	H_2	H_3
MCH06	60	33	23	30.7
MCH09	86	46	32	43.5
MCH10	100	55	32	52.5

Fig. 1 Cross section of MCH/MCL type

Table 1 Combination of stroke and ball screw lead

Model No.	Lead (mm)	Stroke (mm) 50 100 200 300 400 500 600 700 800 900 1 000 1 200 1 400 1 600 1 800
MCH06 MCL06	5 10 20	Standard stock / Made to order
MCH09	5 10 20	
MCH10	10 20	

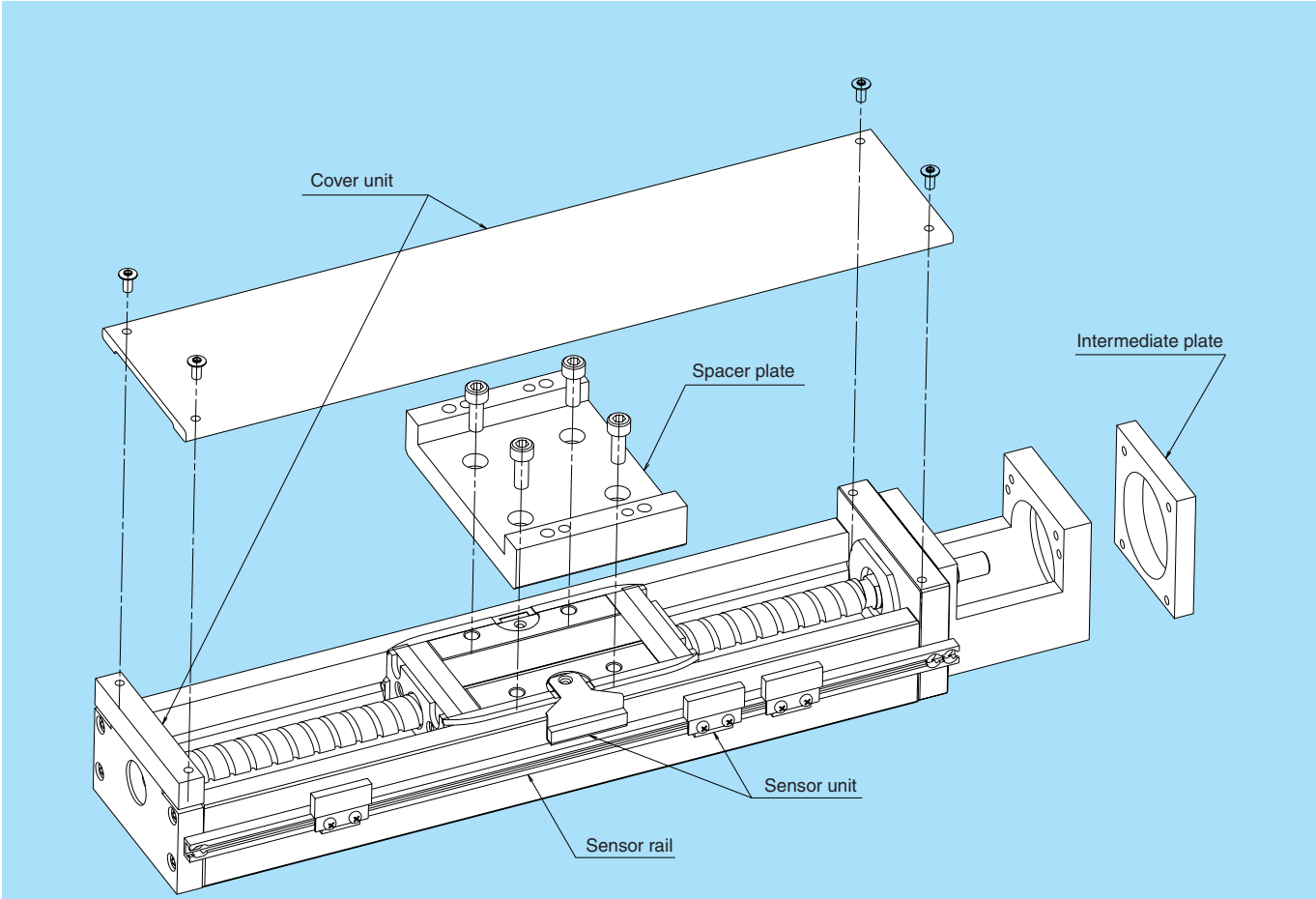

Fig. 2 Optional components

2. Features

(1) High rail rigidity as a beam
This type is designed to enhance rigidity of rail in the extreme. As a result, the rigidity of rail as a beam is approximately three to eight times that of the conventional type (MCM type). Because of its high rigidity, this type is suitable for applications in which the rail itself is used as a part of the structural components. However, this leads to an increase in mass. This increase in mass may be a drawback for applications where light weight is required, such as an end effector. In order to make up for this drawback, MCL06, with a lower rail height than that of MCH06, is provided. The combination of stroke and ball screw lead is shown in Table 1.

(2) Long-term maintenance-free
All MCH and MCL types are equipped with the NSK K1® lubrication unit as standard equipment, same as the conventional MCM type, offering a long-term maintenance-free operation.

When the NSK K1® is equipped, the stroke is shortened by its width. When longer strokes are required, types without the NSK K1® are also available. For more information, please contact NSK.

(3) Variety of optional components
In order to accommodate a wide range of customer needs, a cover unit (including spacer plate), sensor unit, sensor rail, and intermediate plate for various motors are available as optional components. (Refer to Fig. 2)

3. Typical Applications and Coexistence With Conventional Type

The Monocarrier® can be used for all automating systems, such as manufacturing automobile parts, semiconductors, liquid crystal displays, food, and medical instruments. The MCH type is suitable for applications requiring high rigidity of component in a compact composition, while the MCM type is suitable for applications requiring instruments of lightened weight. We think that the range of customer selection is further extended by this sort of series reinforcement.

New Generation of NSK Linear Guides —Miniature PU Series

Miniature PU Series is the new generation of NSK miniature linear guides, consisting of a ball recirculating component made of resin and newly designed ball slide body. This series is recently commercialized with the aim of application to the most advanced technology fields from semiconductor manufacturing systems to medical instruments, by making good use of the various features.

Note that the mounting dimension of the PU Series is interchangeable with that of the conventional miniature LU Series, and the basic load rating for both series is the same. We expect that this series shall be utilized in a more extensive range of applications.

The outline of the PU Series is introduced as follows:

1. Features

(1) The smooth motion of the ball slide is achieved by the smooth circulation of the balls due to new materials and structure of the ball recirculating components.
(2) A resin material is used in a part of the ball slide, reducing ball slide weight by 20% compared to conventional ball slides.
(3) Since the recirculation component is made of resin, noise generation from the impact of balls against the recirculation hole is reduced and a gentler tone is obtained.
(4) A design minimizing dust generation, using such features as the restraint of the stepped portion on the ball raceway and the labyrinth structure, is used all over the ball slide.
(5) The labyrinth between the side face of the rail and the inner wall of the ball slide provides a similar effect as a bottom seal, and achieves superior dustproof protection.
(6) High corrosion resistance is obtained by using stainless steel.
(7) Easy handling, because balls are supported by a retainer and do not fall off, even when a ball slide is removed from a rail.
(8) The NSK K1® lubrication unit can be equipped, offering long-term maintenance-free operation.

2. Accuracy, Preload, and Dimension

There are four accuracy grades: super precision grade P4, high precision grade P5, precision grade P6, and normal grade PN. Two levels of preload, slight preload Z1 and fine clearance Z0, are available. The main dimensions of each model are shown in Table 1.

Photo 1 Appearance of Miniature PU Series

3. Interchangeability With LU Series

The mounting dimensions of the PU Series and the LU Series (LU09TR, LU12TR and LU15AL) are interchangeable with each other and both basic load ratings are the same.

4. Applications

This series is suitable:

- For liquid crystal display manufacturing equipment and printed circuit board manufacturing equipment because of smooth motion properties and low dust generation;
- For semiconductor manufacturing systems (mounter, die bonder, exposure device) because of light weight and low dust generation;
- For medical instruments and various precision stages because of gentle tone and superior dust-proof.

Table 1 Standard dimensions

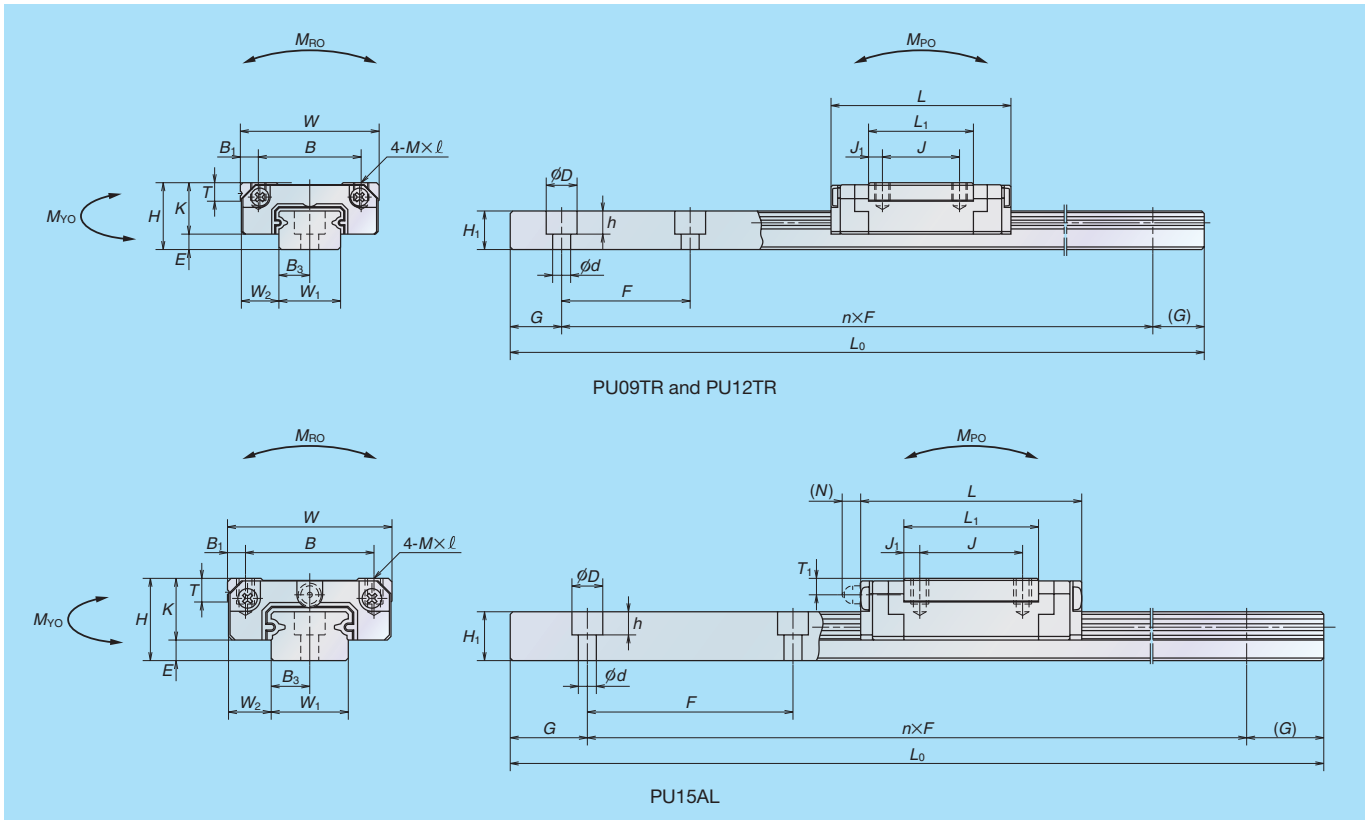

Unit: mm

Model No.	Assembly			Ball slide												
	Height			Width	Length	Mounting tap hole								Grease fitting		
	H	E	W_2	W	L	B	J	M × Pitch × ℓ	B_1	L_1	J_1	K	T	Hole size	T_1	N
PU09TR	10	2.2	5.5	20	30	15	10	$M3 \times 0.5 \times 3$	2.5	19.6	4.8	7.8	2.6	–	–	–
PU12TR	13	3	7.5	27	35	20	15	$M3 \times 0.5 \times 3.5$	3.5	20.4	2.7	10	3.4	–	–	–
PU15AL	16	4	8.5	32	43	25	20	$M3 \times 0.5 \times 5$	3.5	26.2	3.1	12	4.4	ø3	3.2	(3.3)

Model No.	Rail							Basic load rating					Ball diameter	Weight	
	Width	Height	Pitch	Mounting bolt hole		G	Maximum length	Dynamic	Static	Static moment (N·m)				Ball slide	Rail
	W_1	H_1	F	$d \times D \times h$	B_3	(recommended)	L_{0max}	C(N)	C_0(N)	M_{RO}	M_{PO}	M_{YO}	D_W	(g)	(g/100 mm)
PU09TR	9	5.5	20	$3.5 \times 6 \times 4.5$	4.5	7.5	600	1 180	1 770	9	5	5	1.587	16.4	35
PU12TR	12	7.5	25	$3.5 \times 6 \times 4.5$	6	10	800	2 160	2 450	22	12	12	2.381	32.2	65
PU15AL	15	9.5	40	$3.5 \times 6 \times 4.5$	7.5	15	1 000	4 300	4 500	42	22	22	3.175	58.9	105

High Speed and Low Noise Ball Screws HMC-B02 Series

Recently, we have developed and marketed the High Speed and Low Noise Ball Screw HMC-B02 Series for high speed machine tools.

Compared with the current HMC-B01 Series ball screws for high speed machine tools, the new HMC-B02 Series ball screws are innovative products that ensure remarkably higher speed, lower noise, and smaller ball nut body by implementing a newly developed ball recirculating mechanism.

1. Background

Recently, higher speed and higher accuracy of machine tools have seen remarkable gains. In the case of speed increase, rapid traverse speed of 50 to 60 m/min of machining centers is nothing new at present, and the highest speed level reaches 100 m/min or more. It is presumed that this trend of higher speed and higher acceleration/deceleration will continue together with the pursuit of improvement in productivity by reducing cycle time.

For ball screws used under such conditions, improvement in total function of ball screws, such as further increases in speed, decreases in noise level, and downsizing, is strongly required.

2. HMC-B02 Series

In response to market demand, we have developed and marketed the high speed and low noise ball screw HMC-B02 Series, the new ball screws for high speed machine tools, as shown in Photo 1.

The product lineup of the series is shown in Table 1. We are at work on a plan to expand the series.

The HMC-B02 series utilizes a deflector provided inside the ball nut to scoop up balls along their moving direction, instead of using a conventional return tube to recirculate the balls. This mechanism has realized remarkably high speed, low noise, and compactness of ball nut body.

Table 1 Product lineup of series

Unit: mm

Shaft diameter \ Lead	10	16	20	25~30
32	Prospective development	○	○	Prospective development
36		○	○	
40		○	○	
45		○	○	
50		○	○	

Photo 1 HMC-B02 series

3. Features

3.1 High speed

In the case of conventional recirculation mechanisms, due to the repetitive impact of balls on the tip of the recirculation components, the maximum speed of the ball screw depends on the fatigue strength of the tip of the recirculation components.

The new mechanism makes remarkable high speed possible, and the d·N value has reached 180 000 because the recirculation component scoops up balls smoothly into their moving direction. This d·N value represents an improvement of 33% over the conventional maximum value of 135 000. Note that d·N value is a parameter representing speed properties of ball screws, where d is the shaft diameter (mm) and N is the rotational speed (min^{-1}).

3.2 Low noise

The introduction of the above mentioned scoop-up mechanism and the soundproof effect due to recirculation components that are built in a ball nut have realized a gentler tone as well as remarkable low noise. Fig. 1 shows the results of experiments comparing the noise level of the scoop-up mechanism with that of a conventional mechanism. From Fig. 1, it is found that noise level is reduced by 5 to 7dB (A).

3.3 Compactness of ball nut outside diameter

The introduction of the new scoop-up mechanism has downsized ball nut outside diameter by up to 30% compared with the conventional series. Ball nut mounting dimensions conform to DIN (DIN69051) amendment.

3.4 High dustproof properties and low friction of seal

In order to meet application for environments heavily contaminated with foreign materials, the newly developed contact type seals are used in place of conventional labyrinth seals. Compared with a conventional labyrinth seal, results from experiments on the new contact type seal showed that the quantity of contaminant of ball nut is reduced to approximately 1/15 of that of a conventional labyrinth seal.

Generally, a contact type seal has an adverse effect of increase in frictional torque because of sliding contact with the screw shaft, though it does have high dustproof properties. Because the newly developed seal is shaped into a thin plate, the friction between the new contact type seal and the screw shaft is remarkably minimized. In addition, the seal is equipped with scrapers on both sides to prevent a seal from turning up, ensuring high durability.

3.5 Reduction in temperature rise

Specifications of the series include forced cooling through an optional hollow screw shaft, the same as the conventional series.

The problem of heat generation becomes more acute with the realization of high speed and high accuracy. This forced cooling mechanism minimizes temperature rise and shortens the saturating time of temperature rise as well.

In addition, because of the minimizing effect on heat generation due to forced cooling through the hollow shaft, the support bearings on both ends of screw shaft can be a fixed-to-fixed configuration, obtaining high rigidity and high accuracy.

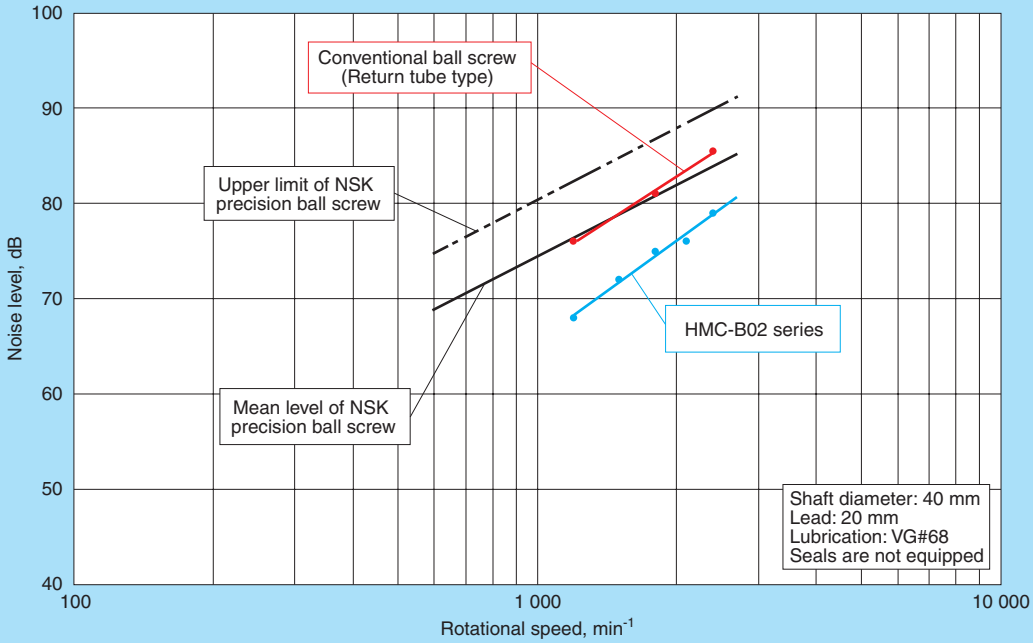

Fig. 1 Comparison of noise levels

SPACEA™ Series YS Bearings for Vacuum Environments

For many years, NSK has been dealing in bearings for vacuum environments, such as for X-ray tubes and vacuum equipment. NSK now offers SPACEA™ series YS bearings for IT related equipment as well. NSK's YS bearings are especially suited for equipment used in the manufacture of semiconductors, liquid crystal displays, hard disks, and other equipment operating in a vacuum environment under relatively high-load conditions compared to other solid lubricants.

1. Bearing Specifications and Features

In the past, vacuum grease-packed bearings, degreased stainless steel bearings, and silver-coated bearings have been used in vacuum environments. Vacuum grease-packed bearings provided sufficient durability to a certain extent. However, this type of bearing risked contamination with oil particle emissions. Degreased stainless steel bearings and silver-coated bearings solved the oil and grease particle contamination problem, but their durability was insufficient.

NSK's YS bearings for vacuum environments have solved all of these conventional-bearing problems by using molybdenum disulfide (MoS_2) solid lubricant. The most outstanding feature of MoS_2-based solid lubricant is that it can bear a relatively high load (P/Cr by approximately 5%) compared to other solid lubricants. The YS bearing for vacuum environments comes in three types: self-lubricating cage type, spacer-joint type, and corrosion resistant type.

(1) Self-lubricating cage type

Fig. 1 illustrates the construction of a self-lubricating cage type YS bearing for vacuum environments. The cage is a composite of resin and MoS_2 for low

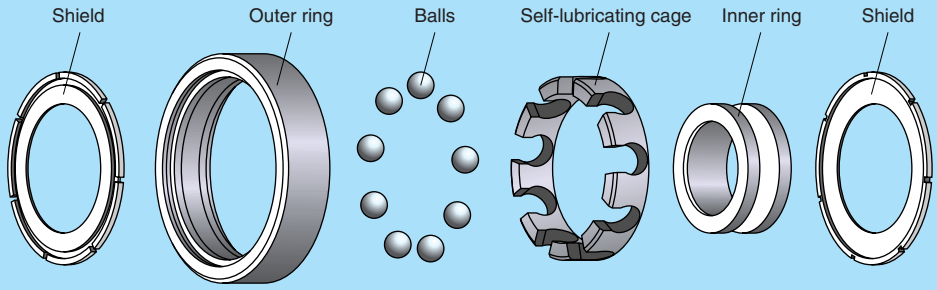

Fig. 1 Construction of YS bearing with self-lubricating cage

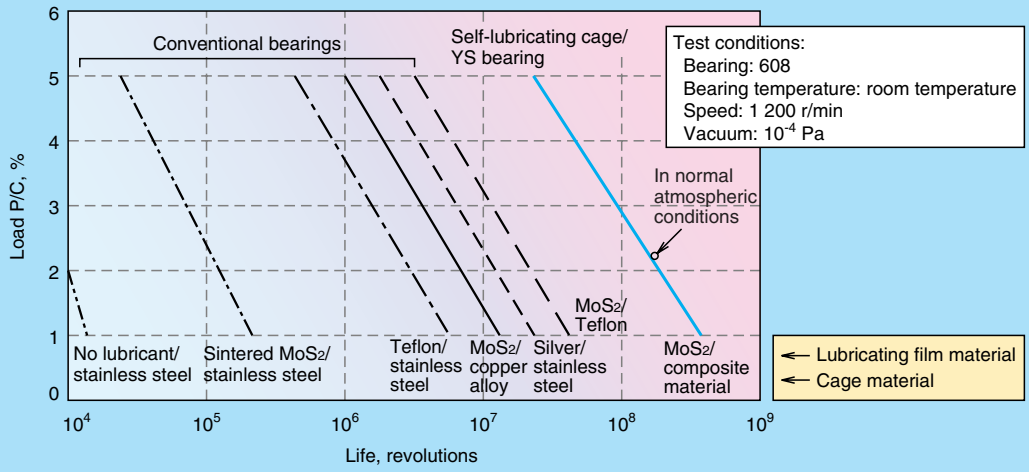

Fig. 2 Comparison of conventional bearings and YS bearings with self-lubricating cage

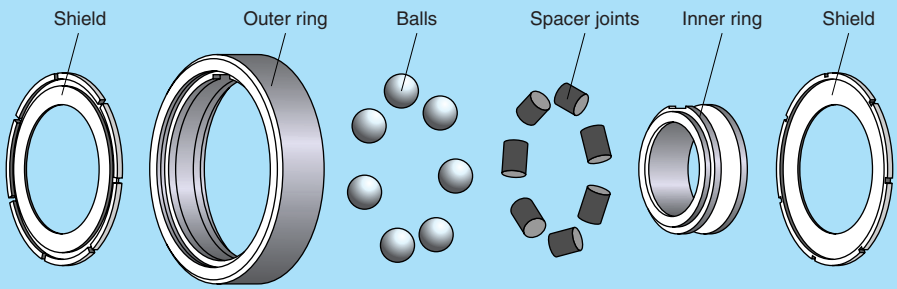

Fig. 3 Construction of YS bearing with spacer joints

outgassing and high heat resistance up to 200˚C. The resin material ensures a stable and long-term supply of solid lubricant on the running surfaces. Ball surfaces are also coated with an MoS_2 film that provides improved initial lubricating properties. Stainless steel is used for components other than the cage in consideration of rust prevention during assembly or maintenance.

Fig. 2 compares the durability of various bearings for vacuum environments. Self-lubricating cage type YS bearings for vacuum environments have 10 times the durability of conventional types. YS bearings show the same remarkable durability for atmospheric environments, making them ideal for oil-free conditions.

(2) Spacer-joint type

Fig. 3 illustrates the construction of spacer-joint type YS bearings operating under high-temperature conditions in a vacuum environment. The spacer joints use an alloy-based material (sintered alloy of refractory metal and MoS_2) and serve as spacers between rolling elements that are also resistant to temperatures as high as 350˚C.

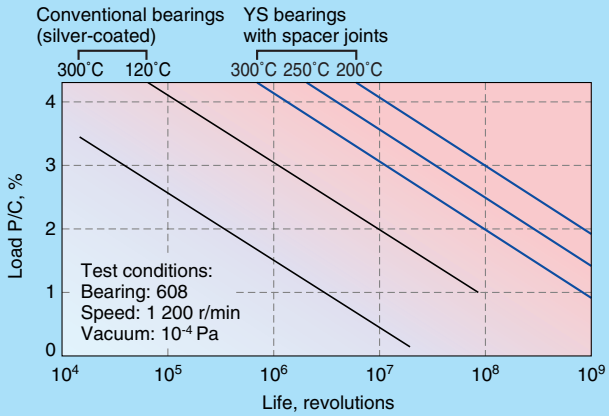

Fig. 4 Comparison of conventional silver-coated bearings and YS bearings with spacer joints

Fig. 4 compares the durability of YS bearings with that of conventional silver-coated bearings. YS bearings with spacer joints, operating under high-temperature conditions for vacuum environments, enjoy 10 times

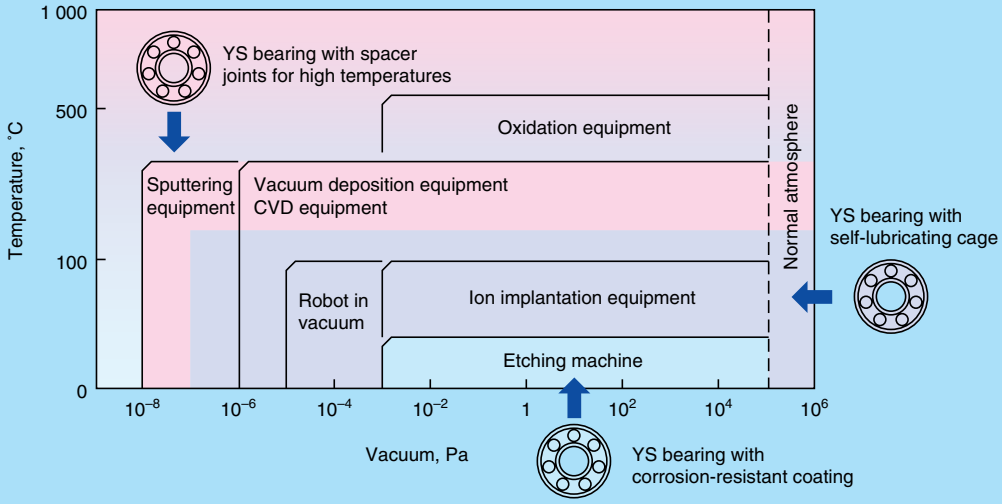

Fig. 5 YS bearing applications in semiconductor manufacturing process

the durability of conventional products.

(3) Corrosion-resistant type
NSK offers a corrosion-resistant type of YS bearing, which is used in processes where halogen gas is introduced into the vacuum. This type of bearing has outer and inner rings that are coated with a nickel-based corrosion-resistant film and includes a self-lubricating cage. Ceramic balls may be used for bearings operating in a corrosive environment.

2. Examples of Applications

Fig. 5 illustrates the applicable range of YS bearings for vacuum environments operating under high-temperature and atmospheric pressure conditions, such as in a semiconductor manufacturing facility. Bearings with a self-lubricating cage meet the needs of a transfer robot in a normal atmospheric environment. Bearings with high-temperature spacer joints are suitable for vacuum deposition equipment and CVD equipment. Bearings with a corrosion-resistant coating are effective in the etching process where corrosive gas is used. In the future, we expect YS bearings with self-lubricating MoS_2-based material to be very useful for robots operating in a vacuum environment where large-sized liquid crystal panel bases are processed.

3. Conclusion

Thanks to the rapid technological innovations of IT related components, we expect an increase in the number of applications taking advantage of our SPACEA™ series YS bearings for vacuum environments in the manufacturing process.

YSB Series Megatorque Motor

NSK Ltd. has been selling the low-price YS Series direct drive motors.

Recently, the demands for higher performance and lower price have grown along with the increase in Megatorque motor applications for diversified industrial fields. To meet such needs, YSB Series Megatorque motor has been newly developed and is introduced as follows:

1. Appearance and specifications

The appearance of the motors is shown in Photo 1 with their specifications in Table 1.

The YSB Series maintains the basic specifications of the conventional YS Series and the height and mounting dimensions are interchangeable with YS Series motors.

The ESB Series of driver unit has also been developed as the dedicated driver unit.

2. Features

(1) Direct drive
The high accuracy positioning without backlash is realized as the motors are capable of mounting load directly and driving it without a mechanical speed reducer.

(2) High accuracy
The position detector (resolver) with a high resolution of 819 200 pulse/revolution is built in the motor. Accordingly, repeatability is enhanced to ± 1.6 sec.

(3) High reliability
As a high rigid bearing (crossed roller bearing) is incorporated into the motor, high reliability and long-term maintenance-free operation are achieved.

(4) High function driver unit
The use of the dedicated ESB Series driver unit provides the functions necessary for motion control.

Photo 1 YSB Series Megatorque Motor

Table 1 Motor specifications

Functional item \ Motor reference number		M-YSB2020KN001	M-YSB3040KN001
Maximum output torque	(N·m)	20	40
Maximum current	(A)	6	6
Maximum speed	(s^{-1})	3	3
Resolution of resolver	(pulse/rotation)	819 200	819 200
Absolute positioning accuracy	(s)	150	150
Repeatability	(s)	±1.6	±1.6
Permissible axial load	(N)	3 700	4 500
Permissible moment load	(N·m)	60	80
Mass	(kg)	10	18
Environmental conditions		Operating temperature 0 to 40˚C, humidity 20 to 80%. Indoor use only. Free from dust, moisture condensation, and corrosive gas. IP30 equivalent.	

- Easy interfacing with various control units that outputs analog command, pulse command, and RS-232C command.
- Smooth rotation without expensive controller is possible because of built-in function of acceleration profiling.
- Field bus option is also available for various networking functions.
  (CC-LINK, PROFIBUS, DeviceNet)

(5) Standard equipment of interchangeable absolute position sensor
Because the absolute position sensor in one turn is built into the motor as standard equipment, homing operation immediately after turning on the power is unnecessary. This interchangeability makes free combination of motor, driver unit, and cable set possible.
* Interchangeability means the possibility of random matching among the same types of motor, drive unit, and dedicated cable set (1 to 30 m in length).

(6) Conformity to overseas safety regulations
Recently, demands to meet various overseas safety regulations have been growing along with an increase in overseas business volume of semi conductor manufacturing equipment, etc.
The combinations of YSB Series motor and ESB Series driver unit comply with UL in the U.S.A. and CE marking in Europe. Accordingly, a machine in which the Megatorque Motor is incorporated can easily comply with safety regulations.

3. Applications and Fields

The Megatorque Motor is used in semiconductor manufacturing systems, liquid crystal display manufacturing systems, machine tools, robots, and various assembling machines and conveying systems. The examples of application are shown in Fig. 1.

4. Conclusion

This commercialized YSB Series Megatorque Motors with built-in absolute position sensor have the same mounting dimensions as the conventional YS Series. In addition, as locating pinholes is standardized, YSB Series motors can easily replace the YS Series motors.

We will release the YSB 4080 and 5120 successively, and will respond to market needs by expanding the YSB Series.

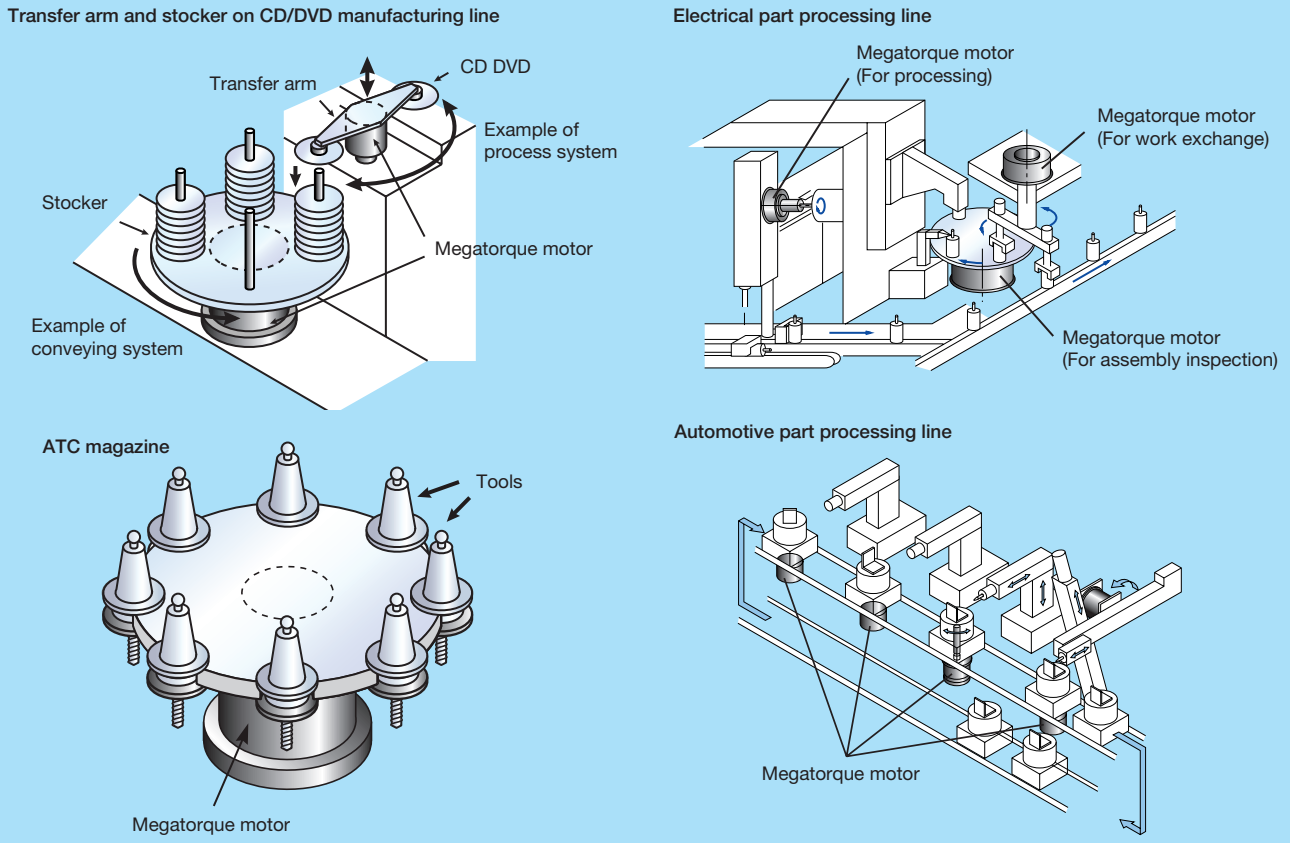

Fig. 1 Examples of application

Worldwide Sales Offices and Manufacturing Plants

NSK LTD.–HEADQUARTERS, TOKYO, JAPAN www.nsk.com
OVERSEAS CS DEPARTMENT — Nissei Bldg., 6-3, Ohsaki 1-chome, Shinagawa-ku, Tokyo 141-8560, Japan
P: 03-3779-7680 F: 03-3779-7433 C: 81
ASIA BUSINESS STRATEGIC DIVISION-HEADQUARTERS — Nissei Bldg., 6-3, Ohsaki 1-chome, Shinagawa-ku, Tokyo 141-8560, Japan
P: 03-3779-7121 F: 03-3779-7433 C: 81

Africa

South Africa:

NSK SOUTH AFRICA (PTY) LTD.
JOHANNESBURG — 25 Galaxy Avenue, Linbro Business Park, Sandton, 2146, Gauteng, P.O. Box 1157, Kelvim, 2054 South Africa
P: (011) 458 3600 F: (011) 458 3608 C: 27

Asia and Oceania

Australia:

NSK AUSTRALIA PTY. LTD. www.nskaustralia.com.au
MELBOURNE — 11 Dalmore Drive, Scoresby, Victoria 3179, Australia
P: (03) 9764-8302 F: (03) 9764-8304 C: 61
SYDNEY — Unit 1, Riverside Centre, 24-28 River Road West, Parramatta, N.S.W. 2150, Australia
P: 02-9893-8322 F: 02-9893-8406 C: 61
BRISBANE — 91 Wellington Road, East Brisbane, Queensland 4169, Australia
P: 07-3393-1388 F: 07-3393-1236 C: 61
ADELAIDE — 64 Greenhill Road, Wayville, South Australia 5034, Australia
P: 08-8373-4811 F: 08-8373-1053 C: 61
PERTH — Unit 4, 36 Port Kembla Drive, Bibra Lake, Western Australia 6163, Australia
P: 089-434-1311 F: 089-434-1318 C: 61

China:

NSK HONG KONG LTD.
HONG KONG — Room 512, Wing On Plaza, Tsim Sha Tsui East, Kowloon, Hong Kong
P: 2739-9933 F: 2739-9323 C: 852

KUNSHAN NSK CO., LTD.
KUNSHAN — 258 South Huang Pu Jiang Rd Kunshan E&T Development Zone Jiang Su 215335, China
P: 0512-5771-5654 F: 0512-5771-5689 C: 86

GUIZHOU HS NSK BEARINGS CO., LTD.
ANSHUN — Dongjiao, Anshun, Guizhou, 561000, China
P: 0853-3521505 F: 0853-3522722 C: 86

NSK (SHANGHAI) TRADING CO., LTD.
SHANGHAI — Room 826, No.1 Ji Long Road, Wai Gao Qiao Free Trade Zone, Shanghai, China
P: 021-62099051 F: 021-62099053 C: 86

NSK REPRESENTATIVE OFFICES www.nsk.com.cn
BEIJING — Room 515, Beijing Fortune Bldg., 5 Dong.san Huan Bei Lu, Chao Yang District, Beijing, 100004, China
P: 010-6590-8161 F: 010-6590-8166 C: 86
SHANGHAI — Room 1005, Shanghai International Trade Center 2200 Yan An Road (w.), Shanghai, 200336, China
P: 21-6209-9051 F: 21-6209-9053 C: 86
GUANGZHOU — Room 2701-02, Guangzhou International Electronics Tower 403, Huan Shi Rd East, Guangzhou, 510095, China
P: 020-8732-0583 F: 020-8732-0574 C: 86
ANSHUN — Dongjiao, Anshun, Guizhou, 561000, China
P: 0853-3522522 F: 0853-3522552 C: 86

India:

RANE NASTECH LTD.
CHENNAI — 14, Rajagopalan Salai, Vallancherry Guduvancherry, Pin-603 202, India
P: 04114-2-66-002 F: 04114-2-66-001 C: 91

NSK REPRESENTATIVE OFFICE
CHENNAI — 2A, First Street, Cenotaph Road, Chennai, 600 018, India
P: 044-2433-4732, 044-2434-3066, 3067 F: 044-2433-4733 C: 91

Indonesia:

PT. NSK BEARINGS MANUFACTURING INDONESIA
JAKARTA PLANT — Blok M-4, Kawasan Berikat, MM2100 Industrial Town Cikarang Barat, Bekasi 17520, Jawa Barat, Indonesia
P: 021-898-0155 F: 021-898-0156, 021-898-0183 C: 62

PT. NSK INDONESIA
JAKARTA — SummitmasII 6th Floor, Jl. Jend. Sudirman Kav. 61-62, Jakarta 12190 Indonesia
P: 021-252-3458 F: 021-252-3223 C: 62

Korea:

NSK KOREA CO., LTD. www.nsk.co.kr
SEOUL — 9F (West Wing) Posco Center 892, Deachi 4 Dong Kangnam-Ku, Seoul, Korea
P: 02-3287-0300 F: 02-3287-0345, 0445 C: 82
CHANGWON PLANT — 60, Songsan-Dong, Changwon, Kyungsangnam-Do, Korea
P: 0551-287-6001 F: 0551-285-9982 C: 82

Malaysia:

NSK BEARINGS (MALAYSIA) SDN. BHD.
KUALA LUMPUR — 1st Floor, Kompleks Kemajuan, No.2, Jalan 19/1B, 46300 Petaling Jaya, Selangor Darul Ehsan, Malaysia
P: 03-7958-4396 F: 03-7958-4412 C: 60
PRAI — 10, Lengkok Kikik 1, Taman Inderawasih, 13600 Prai, Penang, Malaysia
P: 04-399-1763 F: 04-399-1830 C: 60
JOHOR BAHRU — Ground Floor, No. 27, Jalan Bakawali 50, Taman Johor Jaya, 81100 Johor Bahru, Johor, Malaysia
P: 07-354-6290 F: 07-354-6291 C: 60
KOTA KINABALU — Lot 10, Lrg. Kurma 4, Likas Ind. Centre, 5 1/2Miles, Jalan Tuaran, 88450 Inanam Sabah, Malaysia
P: 088-421-260 F: 088-421-261 C: 60

NSK MICRO PRECISION (M) SDN. BHD.
MALAYSIA PLANT — No.43 Jalan Taming Dua,Taman Taming Jaya, 43300 Balakong, Selangor Darul Ehsan, Malaysia
P: 03-961-6288 F: 03-961-6488 C: 60

New Zealand:

NSK NEW ZEALAND LTD. www.nsk-rhp.co.nz
AUCKLAND — 3 Te Apunga Place Mt. Wellington, Auckland, New Zealand
P: (09) 276-4992 F: (09) 276-4082 C: 64

Philippines:

NSK REPRESENTATIVE OFFICE
MANILA — Unit 910 Philippine AXA Life Centre, 1286 Sen. Gil Puyat Avenu, Makati City 1200, Metro Manila, Philippines
P: 02-759-6246 F: 02-759-6249 C: 63

Singapore:

NSK INTERNATIONAL (SINGAPORE) PTE LTD.
SINGAPORE — 48 Toh Guan Road #02-02 Singapore 608837
P: (65) 6273 0357 F: (65) 6275 8937 C: 65

NSK SINGAPORE (PTE) LTD.
SINGAPORE — 48 Toh Guan Road #02-03 Singapore 608837
P: (65) 6278 1711 F: (65) 6273 0253 T: RS24058 C: 65

Taiwan:

TAIWAN NSK PRECISION CO., LTD.
TAIPEI — 9th Fl., 34, Chung Shan N. Rd., Sec. 3, Taipei, Taiwan R.O.C.
P: 02-2591-0656 F: 02-2597-3101 C: 886
TAICHUNG — 107-6, SEC, 3, Wenxin Rd., Taichung, Taiwan R.O.C.
P: 04-2311-7978 F: 04-2311-2627 C: 886

Thailand:

NSK BEARINGS (THAILAND) CO., LTD.
BANGKOK — 25th Floor RS Tower, 121/76-77 Rachadaphisek Road, Dindaeng, Bangkok 10320, Thailand
P: 02-6412150~58 F: 02-6412161 C: 66

NSK BEARINGS MANUFACTURING (THAILAND) CO., LTD.
CHONBURI — 700/430 Moo 7, Amata Nakorn Industrial Estate T. Donhualor, A. Muangchounburi, Chonburi 20000 Thailand
P: (038) 454010~454016 F: (038) 454017, 454020 C: 66

NSK SAFETY TECHNOLOGY (THAILAND) CO., LTD.
CHONBURI — 700/415 Moo 7 Amata Nakorn Industrial Estate T. Donhualor, A. Muang, Chonburi 20000, Thailand
P: (038) 214-317-8 F: (038) 214-316 C: 66

SIAM NSK STEERING SYSTEMS CO., LTD.
CHACHOENGSAO — 90 Moo 9, Wellgrow Industrial Estate, Km. 36 Bangna-Trad Road, Bangwao, Bangpakong, Chachoengsao 24180, Thailand
P: (038) 522-343~350 F: 038-522-351 C: 66

Europe

NSK EUROPE LTD. (EUROPEAN HEADQUARTERS) www.eu.nsk.com
MAIDENHEAD, UK — Belmont Place, Belmont Road, Maidenhead, Berkshire SL6 6TB U.K.
P: 01628-509800 F: 01628-509808 C: 44
NEWARK, UK — Northern Road, Newark, Notts, NG24 2JF U.K.
P: 01636-605123 F: 01636-602750 C: 44

France:

NSK FRANCE S.A.
PARIS — Quartier de l'Europe, 2 Rue Georges Guynemer, 78283 Guyancourt Cedex, France
P: 01 30 57 39 39 F: 01 30 57 00 01 C: 33

Germany:

NSK DEUTSCHLAND GMBH
DÜSSELDORF — Harkortstrasse 15, 40880 Ratingen, Germany
P: 02102-481-0 F: 02102-481-2290 C: 49
STUTTGART — Sielminger Str. 65, 70771 Leinfelden-Echterdingen, Germany
P: 0711-79082-0 F: 0711-79082-289 C: 49
LEIPZIG — Zschortauer Str. 76, 04129 Leipzig, Germany
P: 0341-5631241 F: 0341-5631243 C: 49

NSK STEERING SYSTEMS EUROPE LTD.
STUTTGART — Sielminger Strasse 65 D-70771 Leinfelden-Echterdingen, Germany
P: 0771-79082-277 F: 0771-79082-289 C: 49

NEUWEG FERTIGUNG GMBH
CORPORATE — Ehinger Strasse 5, D-89593 Munderkingen, Germany
OFFICE/PLANT — P: 07393-540 F: 07393-3732 C: 49

Italy:

NSK ITALIA S.P.A.
MILANO — Via Garibaldi, 215 20024 Garbagnate Milanese (Milano), Italy
P: 02-995191 F: 02-99025778, 02-99028373 C: 39

INDUSTRIA CUSCINETTI SPA
TORINO — Via Giotto 4, 10080, S. Benigno C. se, Torino, Italy
P: 0119824811 F: 0119880284 C: 39

Netherlands:

NSK EUROPEAN DISTRIBUTION CENTRE B.V.
De Kroonstraat 38, 5048 AP Tilburg, Nederland
P: 013-4647647 F: 013-4647648 C: 31

Poland:

NSK EUROPE LTD. WARSAW LIAISON OFFICE
WARSAW LIAISON OFFICE — Przedstawicielstowo w Warszawie, ul. Migdalowa 4 lok. 73, 02-796 Warsaw, Poland
P: 022-645-1525, 1526 F: 022-645-1529 C: 48

NSK ISKRA S.A.
CORPORATE OFFICE/PLANT — UL. Jagiellonska 109, 25-734 Kielce, Poland
P: 041-366-5001 F: 041-366-5008 C: 48

NSK EUROPEAN TECHNOLOGY CENTER, POLAND OFFICE
UL. Jagiellonska 109, 25-734 Kielce, Poland
P: 041-366-5812 F: 041-366-5206 C: 48

Spain:

NSK SPAIN S.A.
BARCELONA — Calle de la Hidráulica, 5, P.I. "La Ferrería" 08110 Montcada i Reixac (Barcelona), Spain
P: 093-575-4041 F: 093-575-0520 C: 34

Turkey:

NSK BEARINGS MIDDLE EAST TRADING CO., LTD.
ISTANBUL — Yali Mahallesi, Fevzi Cakmak Caddesi, Caglar Apartman No.11/4, Maltepe 81530, Istanbul, Turkey
P: 0216-442-7106 F: 0216-305-5505 C: 90

United Kingdom:

NSK BEARINGS EUROPE LTD.
OFFICE/MAIN PLANT — 3 Brindley Road, South West Industrial Estate, Peterlee, Co. Durham, SR8 2JD U.K.
P: 0191-586-6111 F: 0191-586-3482 C: 44
FORGE PLANT — Davey Drive, North West Industrial Estate, Peterlee, Co. Durham, SR8 2PW U.K.
P: 0191-518-0777 F: 0191-518-0303 C: 44
NEWARK PLANT — Northern Road, Newark, Nottinghamshire, NG24 2JF U.K.
P: 01636-605123 F: 01636-642083 C: 44
BLACKBURN PLANT — Roman Road Industrial Estate, Blackburn, Lancashire, BB1 2LZ U.K.
P: 01254-661921 F: 01254-679502 C: 44

AEROENGINE BEARINGS UK LTD.
PLANT/SALES — Oldends Lane, Stonehouse, Gloucestershire, GL10 3RH U.K.
P: 01453-822333 F: 01453-825945 C: 44

NSK EUROPEAN TECHNOLOGY CENTRE
NEWARK, UK — Northern Road, Newark, Notts, NG24 2JF U.K.
P: 01636-605123 F: 01636-643241 C: 44

NSK UK LTD.
NEWARK — Northern Road, Newark, Nottinghamshire, NG24 2JF U.K.
P: 01636-605123 F: 0115-940-5419 C: 44

NSK STEERING SYSTEMS EUROPE LTD.
CORPORATE OFFICE/PLANT — Silverstone Drive, Rowiey's Green, Coventry, CV6 6PA U.K.
P: 024-76-588588 F: 024-76-588599 C: 44
PETERLEE COLUMN PLANT — 1 Palmer Road, South West Industrial Estate, Peterlee, Co. Durham, SR8 2JJ U.K.
P: 0191-518-6800 F: 0191-518-6808 C: 44
PETERLEE EPAS PLANT — 6/7 Doxford Drive, South West Industrial Estate, Peterlee, Co. Durham, SR8 2RL U.K.
P: 0191-518-6400 F: 0191-518-6421 C: 44

North and South America

NSK AMERICAS, INC. (AMERICAN HEADQUARTERS)
ANN ARBOR, USA — 4200 Goss Road, P.O. Box 134007, Ann Arbor, MI 48113-4007
P: 734-913-7500 F: 734-913-7511 C: 1

Argentina:

NSK ARGENTINA SRL
BUENOS AIRES — Calle San Lorenzo, 4292-Munro-Buenos Aires-Argentina
P: 011-4762-6556 F: 011-4762-6466 C: 54

Brazil:

NSK BRASIL LTDA. www.br.nsk.com
SÃO PAULO — Rua Treze de Maio, 1633-14° andar-Bela Vista São Paulo-SP, Brazil 01327-905
P: 011-3269-4723 F: 011-3269-4720 C: 55
SUZANO PLANT — Av. Vereador João Batista Fitipaldi, 66-Vila Maluf Suzano-SP, Brazil 08685-000
P: 011-4741-4090 F: 011-4748-2355 C: 55
BELO HORIZONTE — Rua Ceará, 1431-4° andar-sala 405-Funcionários Belo Horizonte-MG, Brazil 30150-311
P: 031-3274-2477 F: 031-3273-4408 C: 55
JOINVILLE — Rua Blumenau, 178-sala 910-Centro Joinville-SC, Brazil 89204-250
P: 047-422-5445/433-3627 F: 047-422-2817 C: 55
PORTO ALEGRE — Av. Cristovão Colombo, 1694-sala 202-Floresta Porto Alegre-RS, Brazil 90560001
P: 051-3222-1324/3346-7851 F: 051-3222-2599 C: 55
RECIFE — Av. Conselheiro Aguiar, 2738-6° andar-conj. 604-Boa Viagem Recife-PE, Brazil 51020-020
P: 081-3326-3781 F: 081-3326-5047 C: 55

Canada:

NSK CANADA INC. www.ca.nsk.com
HEAD OFFICE — 5585 McAdam Road, Mississauga, Ontario L4Z 1N4, Canada
P: 905-890-0740 F: 905-890-0434 C: 1
MONTREAL — 2150-32E Avenue, Lachine, Quebec H8T 3H7, Canada
P: 514-633-1220 F: 514-633-8164 C: 1
TORONTO — 5585 McAdam Road, Mississauga, Ontario L4Z 1N4, Canada
P: 905-890-0561 F: 905-890-1938 C: 1
EDMONTON — 9267-41st Avenue, Edmonton, Alberta T6E 6R5, Canada
P: 604-294-1151 F: 604-294-1407 C: 1
VANCOUVER — 3353 Wayburne Drive, Burnaby, British Columbia V5G 4L4, Canada
P: 604-294-1151 F: 604-294-1407 C: 1

Mexico:

NSK RODAMIENTOS MEXICANA, S.A. DE C.V. www.mx.nsk.com
MEXICO CITY — Minas Palacio No.42-6, Col. San Antonio Zomeyucan Naucalpan de Juarez, C.P. 53750 Estado de Mexico, Mexico
P: 5-301-2741, 5-301-3115, 5-301-4762 F: 5-301-2244, 5-301-2865 C: 52

United States of America:

NSK CORPORATION www.nsk-corp.com
[CORPORATE OFFICE, Aftermarket Business Unit, OEM Business Unit]
ANN ARBOR — 4200 Goss Road, P.O. Box 134007, Ann Arbor, MI 48113-4007
P: 734-913-7500 F: 734-913-7510 C: 1

[BRANCHES and DISTRIBUTION CENTERS]
LOS ANGELES — 13921 Bettencourt Street, Cerritos, California 90703, U.S.A.
P: 562-926-2975 F: 562-926-3553 C: 1
INDIANAPOLIS — 1581 S. Perry Road, Plainfield, Indiana 46168, U.S.A.
P: 317-837-8879 F: 317-837-7207 C: 1
ATLANTA — 5575 Gwaltney Drive, Atlanta, Georgia 30336, U.S.A.
P: 404-349-2888 F: 404-349-1209 C: 1

[PLANTS]
ANN ARBOR — 5400 South State Road, Box 990, Ann Arbor, Michigan 48108, U.S.A.
P: 734-996-4400 F: 734-996-4707 C: 1
CLARINDA — 1100 North First Street, Clarinda, Iowa 51632, U.S.A.
P: 712-542-5121 F: 712-542-4905 C: 1
FRANKLIN — 3400 Bearing Drive, Franklin, Indiana 46131, U.S.A.
P: 317-738-5000 F: 317-738-4310 C: 1
LIBERTY — 1112 East Kitchel Road, Liberty, Indiana 47353, U.S.A.
P: (765) 458-5000 F: (765) 458-7832 C: 1

NSK AMERICAN TECHNICAL CENTER
ANN ARBOR — 4200 Goss Road, P.O. Box 134007, Ann Arbor, MI 48113-4007
P: 734-913-7500 F: 734-913-7852 C: 1

NSK PRECISION AMERICA, INC. www.npa.nsk.com
CHICAGO — 2171 Executive Drive, Suite 100 Addison, Illinois 60101-5600, U.S.A.
P: 630-620-8500 F: 630-620-8555 C: 1
SAN JOSE — 780 Montague Expressway, Suite 508, San Jose, CA 95131
P: 408-944-9400 F: 408-944-9405 C: 1

NSK STEERING SYSTEMS AMERICA, INC. www.nastech.nsk.com
CORPORATE OFFICE/PLANT — 110 Shields Drive Route 2, Box 0030, Bennington, Vermont 05201-8309, U.S.A.
P: 802-442-5448 F: 802-442-2253 C: 1
SALES OFFICE — 4200 Goss Road, P.O. Box 134007, Ann Arbor, MI 48113-4007
P: 734-913-7500 F: 734-913-7328 C: 1

NSK LATIN AMERICA, INC. www.latinamerica.nsk.com
MIAMI — 2500 NW 107 Avenue, Suite 300, Miami, Florida, 33172, U.S.A.
P: (305) 477-0605 F: (305) 477-0377 C: 1

P: Phone F: Fax T: Telex C: Country Code

Printed in Japan

Motion & Control

No.14 May 2003

Published by NSK Ltd.